

University Mohamed Khider – Biskra
Faculty of Sciences and Technology
Departement of Civil Engineering and
Hydraulics



جامعة محمد خيضر - بسكرة
كلية العلوم والتكنولوجيا
قسم الهندسة المدنية والري

Ref :...../2024

المرجع :/2024

Master Project
Specialty: Structures

Title:

Seismic vibration control of nonlinear structures using semi-active dampers

Student:
Rahal Sara

Supervisor:
Dr Abdeddaim Mahdi

Promotion of June 2024

Acknowledgments

All praises to ALLAH almighty, the most gracious and merciful, for giving us strength and endurance to complete this modest work.

We would like to express our immense gratitude to my supervisor, **Dr Abdeddaim Mahdi**, for being there from the start to the end, providing me with inestimable guidance and constant assistance. May ALLAH bless him for all the contributions he has made.

We owe a special thanks to the board of examiners for reading, examining and evaluating our modest work. Last but not least, we are thankful to all our teachers in the department of civil Engineering and our colleagues.

Dedication

I dedicate my work to all my family members and my friends.

A special feeling of gratitude to my loving parents, **Yehya** and **Hakima**, whose affection, love, encouragement and prayers make me able to get such success and honor.

To the memory of my brothers and closest ones to my heart, **Djaber** and **Yazid**, who passed away before I could share this joy with them, may my Lord bless their souls.

To my brothers, sisters, nephews and nieces.

Abstract

Earthquakes are well-known destructive phenomena that constitute a challenge for structural engineers. It is well established that preventing structural damages during seismic events will prevent life and economical losses. For this particular purpose, researchers developed a multitude of vibration control devices and strategies and applied them in real structures with the aim of safeguarding these later during earthquakes. One of the most studied vibration control devices is the magnetorheological (MR) damper. This device is considered as semi-active damper and has the ability to adjust the viscosity of its fluids through a magnetic field, therefore adjusting its control force. The magnetic field in a MR damper can be generated using a small battery. A common point among the previous research works investigating the performance of MR dampers is the assumption of linear structure models. However, it is well established that such an assumption will lead to an overestimation of the damper performance since all the structures will undergo nonlinear deformations when subjected to earthquakes. This work aims to assess the performance of MR dampers in controlling the response of seismically excited nonlinear buildings. The nonlinearity is represented through a Bouc-Wen hysteresis model, which introduces a hysteresis restoring force that is applied to each floor of the studied building. Hence, a multi-story nonlinear building is equipped with MR dampers following various distributions and under various voltage values. The building is then subject to a set of four ground motions, and various dynamic parameters of interest are investigated. The obtained results show a good performance of the MR damper, especially when distributed along all the building floors with a high voltage applied. Further, the MR damper reduces the nonlinear hysteresis force that develops in the building due to earthquake loadings. Hence, this master project contributes to the assessment of nonlinear structural behavior and its seismic control.

Key words: semi-active control, magnetorheological damper, nonlinear structures, seismic excitation, Bouc-Wen model.

المخلص

الزلازل هي ظواهر طبيعية مدمرة حيث تشكل تحدياً للمهندسين الإنشائيين. ومن المعروف أن منع الأضرار الهيكلية أثناء الزلازل يمنع الخسائر في الأرواح والأضرار الاقتصادية. ولهذا الغرض بالذات، قام الباحثون بتطوير العديد من أجهزة واستراتيجيات التحكم في الاهتزازات الزلزالية وتم تطبيقها في هياكل حقيقية بهدف حمايتها لاحقاً أثناء الزلازل. أحد أكثر أجهزة التحكم في الاهتزازات التي تمت دراستها هو المخدم النصف نشط ذو السائل الممغنط. يعتبر هذا الجهاز بمثابة مخدم شبه نشط وله القدرة على تعديل لزوجة سوائله من خلال تطبيق مجال مغناطيسي وبالتالي ضبط قوة المقاومة الخاصة به. يمكن توليد المجال المغناطيسي في المخدم المدروس باستخدام بطارية صغيرة، حيث لا يحتاج إلى طاقة كبيرة لتشغيله. هناك نقطة مشتركة بين الأعمال البحثية السابقة التي تبحث في أداء المخدمات الزلزالية وهي افتراض نماذج ذات مرونة خطية للبنى المدروسة. ومع ذلك، فمن الثابت أن مثل هذا الافتراض سيؤدي إلى المبالغة في تقدير أداء المخدم نظراً لأن جميع الهياكل ستخضع لتشوهات غير خطية عند تعرضها للزلازل. يهدف هذا العمل إلى تقييم أداء مخدم نصف نشط ذو سائل ممغنط في التحكم في استجابة المباني غير الخطية المعرضة للزلازل. يتم تمثيل المرونة اللاخطية في البنية من خلال نموذج بوك-وان (Bouc-Wen) الذي يحاكي قوة الاستعادة المتباطئة المطبقة في كل طابق من المبنى المدروس. ومن ثم، تم تجهيز مبنى ذو مرونة غير خطية متعدد الطوابق بمخدمات نصف نشطة ذات سائل ممغنط تتبع توزيعات مختلفة وتحت قيم جهد كهربائي مختلفة، حيث يتم إخضاع المبنى لأربعة زلازل ويتم فحص معاملات الاستجابة الديناميكية المختلفة ذات الأهمية. أظهرت النتائج التي تم الحصول عليها أداء جيد للمخدم المستعمل خاصة عند توزيعه على جميع طوابق المبنى مع تطبيق الجهد الكهربائي عالي. علاوة على ذلك، يعمل المخدم المستعمل على تقليل قوة الاستعادة المتباطئة الغير الخطية التي تتطور في المبنى بسبب أحمال الزلازل. يساهم هذا المشروع الدراسي في تقييم السلوك الهيكلي غير الخطي ومدى فاعلية التحكم في استجابته الزلزالية.

كلمات مفتاحية: التحكم النصف نشط، مخدم ذو سائل ممغنط، بنية ذات مرونة لا خطية، تحريض زلزالي، نموذج بوك-وان

Summary

Title	Page
Summary	I
List of Figures	IV
List of Tables	VI
General introduction	01
Chapter I Literature review on vibration control systems	
I.1. Introduction	03
I.2. Passive control systems	03
<i>I.2.1. Passive control with base isolation (seismic isolators).</i>	04
<i>I.2.1.1 High damping rubber bearing seismic isolator (HDR)</i>	04
<i>I.2.1.2 Low Damping Natural and Synthetic Rubber Systems</i>	05
<i>I.2.1.3 Lead Rubber Bearing (LRB)</i>	05
<i>I.2.1.4 Friction Pendulum Sliding (FPS) Bearing</i>	06
<i>I.2.2 Passive control with energy dissipators</i>	07
<i>I.2.2.1. Hysteretic devices</i>	07
<i>I.2.2.2. Viscoelastic Shock Absorbers</i>	08
<i>I.2.2.3. Viscous fluid shock absorbers</i>	09
<i>I.2.2.4. Tuned Mass Damper (TMD)</i>	09
<i>I.2.2.5. Tuned Liquid Damper</i>	09
I.3. Active control systems	10
<i>I.3.1 Active Tendon Damper</i>	10
<i>I.3.2. Active Brace System</i>	11
<i>I.3.3. Active Mass Damper Systems</i>	11
I.4. Semi-active control systems	11
<i>I.4.1. Electrorheological Dampers</i>	12
<i>I.4.2. Magnetorheological Dampers</i>	13
<i>I.4.2.1. Rheological models of the MR damper</i>	14
I.5. Hybrid control systems	15
<i>I.5.1. Hybrid Mass Dampers</i>	16
<i>I.5.2. Hybrid Base-Isolation System</i>	17
I.6. Conclusion	17

Chapter II: The nonlinear behavior of structures

II.1. Introduction	19
II.2. Literature review	19
II.3. Basic Concepts of Nonlinear Phenomena	20
<i>II.3.1. Types of nonlinearities</i>	21
<i>II.3.1.1. Geometric nonlinearity</i>	21
<i>II.3.1.2. Material nonlinearity</i>	22
II.4. Inelastic Analysis of Dynamic Response	22
<i>II.4.1. Inelastic Domain</i>	22
<i>II.4.2. Hysteretic Response</i>	23
<i>II.4.3. Mathematical Model of Hysteresis</i>	24
II.5. Mathematical formulation of the material nonlinearity of structures using Bouc-Wen model	25
II.6. Conclusion	27

Chapter III: Mathematical modeling

III.1. Introduction	29
III.2. Assumptions and Limitations	29
III.3. Mathematical Model and Equations of Motion	29
<i>III.3.1. Linear system with a single degree of freedom</i>	29
<i>III.3.2. Nonlinear system with a single degree of freedom</i>	30
<i>III.3.3. Nonlinear system with a single degree of freedom with control device</i>	31
<i>III.3.4. Nonlinear system with multiple degrees of freedom with control device</i>	32
III.4 System Resolution using State Representation (State Space)	35
III.5. Numerical resolution using MATLAB	37
III.6. Conclusion	40

Chapter IV: Numerical study

IV.1. Introduction	42
IV.2. Structural and damper parameters	42
IV.3. Different investigated control strategies	42
IV.4. Description of seismic excitations	44
IV.5. Results and discussion	46
<i>IV.5.1. Peak top floor displacement and time history under various control strategies</i>	46
<i>IV.5.2. Base shear at the base</i>	50

<i>IV.5.3. Peak drift values of all the floors under different control strategies</i>	52
<i>IV.5.4. Peak inter-story drift under different control strategies</i>	54
<i>IV.5.5. Peak MR damper force</i>	56
<i>IV.5.6. Peak restoring force of the first floor under various control strategies</i>	57
<i>IV.5.7. Hysteresis Loop</i>	58
IV.6. Conclusion	59
General conclusion	62
Bibliographic reference list	63

List of figures

Figure title	Page
Figure I.1. Structural control systems	03
Figure I.2 Passive vibration damping	04
Figure I.3: construction of high damping rubber bearing	04
Figure I.4: Lead Rubber Bearing	05
Figure I.5: Friction pendulum system	06
Figure I.6. Friction pendulum bearing	06
Figure I.7: Metallic damping devices	07
Figure I.8: a) Installation of Sumitomo friction damper in steel frame b)Energy Dissipating Restraint c)Uniaxial friction damper d)Pall Friction Damper	08
Figure I.9: Typical solid VE damper	08
Figure I.10: Cylindrical container fluid damper from GERB	09
Figure I.11: Pendulum tuned mass damper	09
Figure I.12: Active Control System	10
FigureI.13:Schematic diagram of active tendon system	10
FigureI.14:Active bracing system with hydraulic actuator	11
FigureI.15: Schematic Active Mass Damper (AMD)	11
FigureI.16:Semi-Active Control System	12
Figure I.17:Schematic of an Electrorheological Fluid Damper	13
FigureI.18: a) Magnetorheological fluid b) Magnetorheological fluid Damper	13
Figure I.19: Simple Bouc-Wen model for MR dampers	14
Figure I.20: Modified Bouc-Wen model for MR dampers	15
Figure I.21: Hybrid Control Systems	16
Figure I.22:The schematic diagram of the hybrid mass damper system	16
Figure I.23:a) Hybrid Base-Isolation system with MR damperb) Hybrid Base- Isolation system with actuators	17
Figure II.1: Linearity in structural systems	21
Figure II.2: Structural system requiring geometric nonlinear analyses	22
Figure II.3: Material (a) linear elastic, (b) nonlinear elastic and (c) inelastic	22
Figure II.4: effect of loading and unloading with reversal of the direction of effort	23
Figure II.5: Force-strain curve for an inelastic material	23
Figure II.6:Model of Hysteresis	24

Figure II.7: Force-strain curve for an elastoplastic material	24
Figure II.8: Energy dissipation in an elastoplastic system	25
Figure II.9: Bouc-Wen model principle of functioning	26
Figure II.10: Various hysteresis loop shapes obtained under different parameters	26
Figure III.1: Equivalent system of Linear system with a single degree of freedom	30
Figure III.2: Free body diagram of Linear system with a single degree of freedom	30
Figure III.3: Equivalent system of linear system with a single degree of freedom	30
Figure III.4: Free body diagram of -linear system with a single degree of freedom	31
Figure III.5: Equivalent system of Nonlinear system with a single degree of freedom with control device	31
Figure III.6: Free body diagram of Nonlinear system with a single degree of freedom with control device	31
Figure III.7: Nonlinear shear frame structure equipped with MR dampers	32
Figure III.8: Equivalent system of Nonlinear system with multiple degrees of freedom with control device located at first and last floors	33
Figure III.09: Free body diagram of Nonlinear system with multiple degrees of freedom with control device	33
Figure III.10; Block-diagram representation of a state-space model	36
Figure III.11: Simulink file of the used model for a SDOF case	38
Figure III.12: The MR damper diagram modeled in SIMULINK	38
Figure III.13: Modified Simulink MR Bouc-Wen shock absorber file	39
Figure III.14: The nonlinear diagram modeled in SIMULINK	39
Figure III.15: MATLAB resolution diagram	40
Figure IV.1: Various control strategies (a) all floors, (b) odd floors, (c) even floors	43
Figure IV.2: Earthquakes record used in this study	45
Figure IV.3: Time history of Top floor displacement under various control strategies	49
Figure IV.4: Base shear at the base under different control strategies	52
Figure IV.5. Peak drift values of all the floors under different control strategies	54
Figure IV.6: Peak inter-story drift under different control strategies	56
Figure IV.7: hysteresis loop in terms of relative velocity	58
Figure IV.8: hysteresis loop in terms of displacement	59

List of tables

Table title	Page
Table IV.1: The properties of the primary structure	43
Table IV.2: Nonlinear model parameters	44
Table IV.3: The properties of MR damper	44
Table IV.4: Peak displacement under various control strategies [m]	46
Table IV.5: Maximum base shear [kN]	50
Table IV.6: Peak MR damper force [kN]	56
Table IV.7: Maximum restoring force [kN]	57

General introduction

General Introduction

In recent years, seismic activity has caused enormous human and material losses, which has motivated several researchers to introduce new strategies for controlling seismic vibrations in order to protect structures, thus reducing losses due to earthquakes. These control strategies can be passive, active, semi-active or hybrid; this later consists of a combination of two or more control strategies. Among the most reliable devices, the magnetorheological damper is the most studied. However, it is important to take into account the nonlinearity of the structure. Thus, any structure subjected to seismic acceleration is subjected to irreversible nonlinear deformations. Therefore, it is important to take into consideration the nonlinear behavior of a structure when modeling it but also the effect of the introduction of control devices. This consideration is often omitted when studying devices which usually result in overestimation of the control device performance.

The main objective of this work is to study the effect of the introduction of semi-active control devices on the nonlinear behavior of a structure subjected to seismic loading. A medium-high structure is used for this purpose. The rigidity of the structure is partitioned into two parts, one pre-plastic and the other post-plastic components estimated using a Bouc-Wen hysteresis model. The seismic response values observed will be the top floor displacement, the drift and inter-story drift, the shear forces, the peak damper force and the hysteretic behavior of the stiffness elements.

This work consists of four chapters, the contents of which are briefly described below:

The first chapter This section presents an overview of passive, semi-active, active and hybrid vibration control systems. For each system, descriptions, diagrams, and various types will be provided. This chapter aims to provide the reader with an overview of the latest advancements in vibration control technologies.

The second chapter deals a review of literature on the nonlinear behavior of structures and Mathematical formulation of the material nonlinearity of structures. This chapter examines the importance of modeling hysteretic behavior in structures, especially in the context of seismic analysis and design. Also, the model to be used for representing the nonlinear behavior of the studied structure will be chosen and detailed mathematical-wise.

The third chapter This section provides an overview of the mathematical formulation and numerical resolution of a dynamic system using state space representation. It includes the

description and assumptions necessary for validating the state space method and defines its general form. Additionally, examples of solving dynamic systems in state space for both single degree of freedom and multiple degrees of freedom are presented. The numerical solutions are demonstrated using MATLAB and SIMULINK module.

The fourth chapter: This section addresses the numerical study of an eight-story nonlinear building equipped with an MR damper. The system's simulation under various earthquake excitations is conducted using MATLAB. This chapter presents the parameters of the structure, including the nonlinear coefficients, and details the earthquake records used. The MR damper parameters and various locations and voltages adopted. The results are analyzed in terms of displacement at the top of the building, shear force at the base, maximum drift, inter-story displacement, the maximum force produced by the MR damper, and hysteresis force and loops. These findings are illustrated through tables and figures.

The master project concludes with a general conclusion, highlighting the main findings of this work and offering recommendations for future research projects.

Chapter I: Literature review on vibration control systems

Chapter I: Literature review on vibration control systems

I.1. Introduction

In recent years, vibration control strategies have become a source of interest in order to protect structures against damage and dynamic actions[1]. Therefore, after construction, it is necessary to safeguard structures with protection systems, reducing their dynamical response. Among the widely used control methods, four different approaches can be distinguished namely, passive, active, semi-active, and a fourth one, which is hybrid control(Figure I-1).

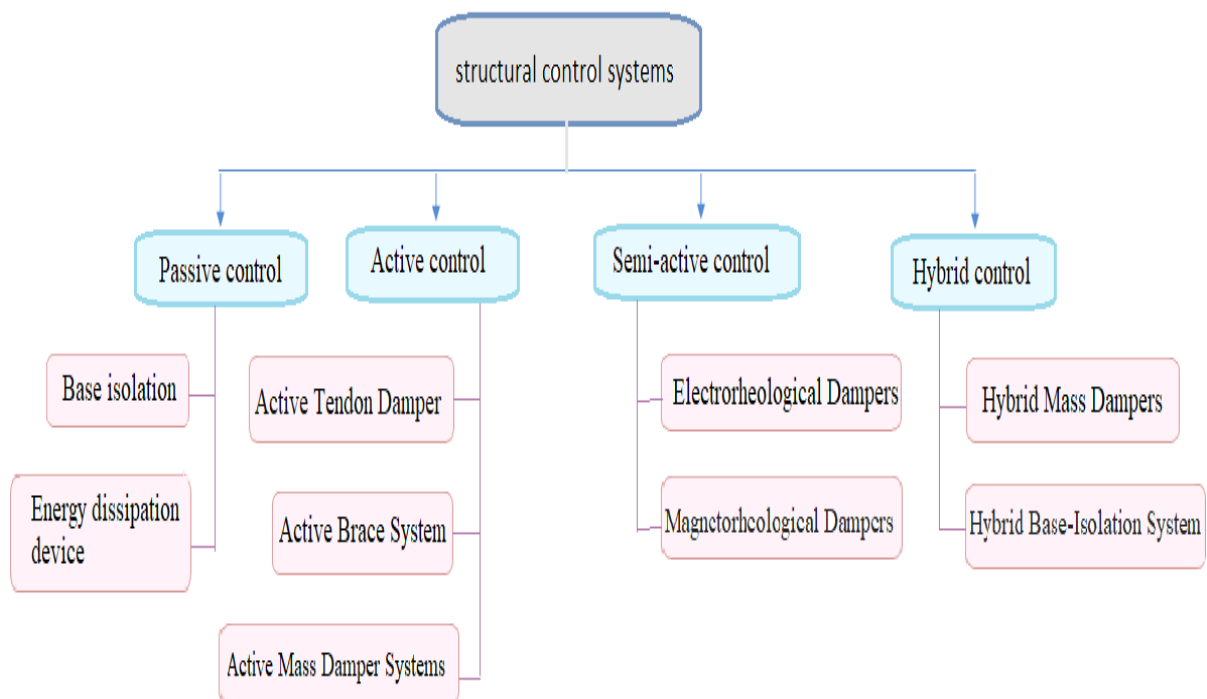


Figure I.1. Structural control systems

I.2. Passive control systems

Passive control involves equipping the structure with a device that dissipates energy or filters the transmission of forces within the structure[2]. The integration or addition of systems with damping properties, coupled to the structure in such a way that structure vibrations are passively dampened, requires no external energy source (Figure I.2). In passive control, mass, damping, stiffness, or their combination are altered by adding components to the structure. These components are activated by the movements of the structure and provide control forces based on their dynamic characteristics. Primarily, there are two categories of passive systems: base seismic isolation and energy dissipation system.

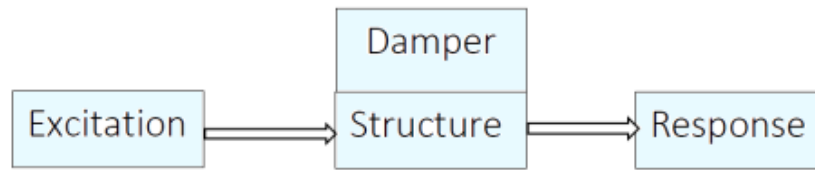


Figure I.2 Passive vibration damping [3]

I.2.1. Passive control with base isolation (seismic isolators).

Elastomeric isolators are constructed from rubber or neoprene reinforced with steel plates, offer lateral flexibility with steel reinforcement preventing elastomer swelling and ensuring vertical stiffness. Their working principle is to decouple the motion of the ground from that of the super-structure. Common types include low-damping isolators (LDR and HDR), elastomeric base isolator with lead core (LRB), and friction pendulum isolator (FPS).

I.2.1.1 High damping rubber bearing seismic isolator (HDR)

The term HDR is applied to elastomeric supports where the elastomer used provides a significant amount of damping, typically ranging from 8% to 15% of critical damping. A high damping rubber isolator consists of multiple layers of rubber with high damping properties separated by steel plates to increase vertical stiffness (Figure I.3). It is vertically rigid, capable of supporting vertical gravity loads while being laterally flexible, allowing for large horizontal displacements. Through its flexibility and energy absorption capabilities, the HDR system reflects and partially absorbs some of the earthquake energy before it can be transmitted to the structure.



Figure I.3: construction of high damping rubber bearing[4]

1.2.1.2 Low Damping Natural and Synthetic Rubber Systems

Low Damping Natural and Synthetic Rubber Bearings (LDRB) are widely used in Japan along with additional damping devices such as viscous dampers, steel bars, lead bars, and friction devices. These isolators consist of two thick steel end plates and numerous steel shims. The rubber is vulcanized and bonded to the steel in a single operation, providing high vertical stiffness while the low shear modulus of the elastomer controls horizontal stiffness. The material behaves linearly in shear up to stresses exceeding 100%, with damping ranging from 2% to 3% of critical damping. It is not prone to creep, ensuring long-term stability.

The advantages of these low damping elastic laminated bearings include simplicity in manufacturing, ease of shaping, and a mechanical response unaffected by rate, temperature, layers, or aging. However, the drawback is the need for additional damping systems, requiring sophisticated connections and susceptibility to low-cycle fatigue in the case of metallic dampers.

1.2.1.3 Lead Rubber Bearing (LRB)

The Elastomeric Base Isolator with Lead Bar (LRB) is a crucial type of base isolation system, extensively studied, and implemented globally in numerous buildings. The LRB isolator, is composed of alternating layers of rubber and steel for stability, structural support, and vibration isolation (Figure I.4). It features a central lead core to enhance damping effects, providing stiffness under normal loads and dissipating energy during high lateral loads. The isolator is further equipped with upper and lower steel plates to secure the building and prevent sliding movement across its foundation.

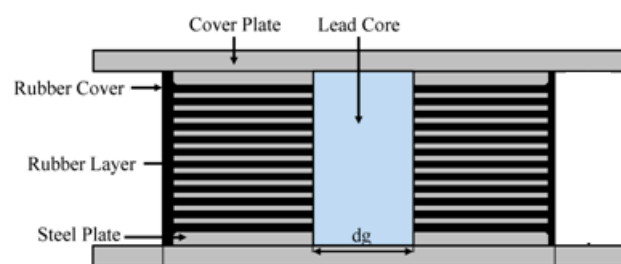


Figure I.4: Lead Rubber Bearing[5]

The Elastomeric Base Isolator with Lead Bar is rather flexible horizontally but quite rigid vertically. The horizontal stiffness of the support is also designed to withstand wind forces with little to no deformation. It not only supports vertical loading but also extends the seismic

response period of the structure, providing isolation and energy dissipation. The recommended normal period for optimal performance is between 1.5 and 2.5 seconds

1.2.1.4 Friction Pendulum Sliding (FPS) Bearing

The combination of sliding bearings and a pendulum-type response gives rise to an intriguing seismic isolation system known as a Friction Pendulum System (FPS), illustrated in Figure I.5. In FPS, isolation is accomplished through an articulated slider on a spherical, concave chrome surface.

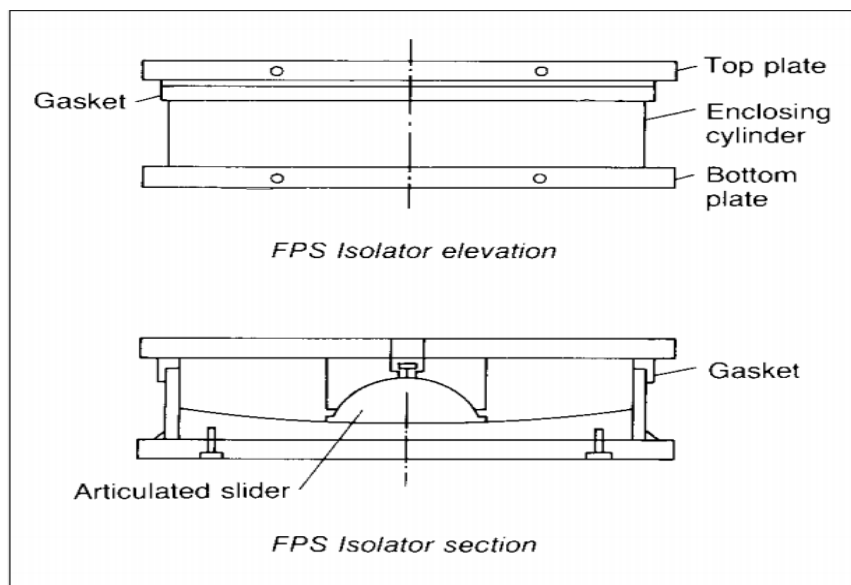


Figure I.5: Friction pendulum system[6]

A friction pendulum bearing during various functioning phases is shown in Figure I.6. These bearings shield the structure from seismic energy by using a pendulum. Typically, a steel ball that rests on a curved surface serves as a pendulum. The pendulum swings back and forth during an earthquake, dissipating the energy of the seismic waves

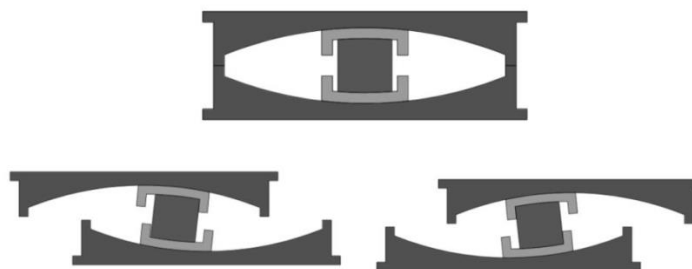


Figure I.6. Friction pendulum bearing [7]

1.2.2 Passive control with energy dissipators

Energy dissipators are engineered systems intended to absorb a portion of the seismic energy, preventing dissipation through inelastic deformations in structural elements. They come in various types, including hysteretic, viscoelastic, and viscous fluid dampers. Hysteretic dissipators rely on steel yielding and friction, mainly influenced by displacements. Viscoelastic dissipators, whether solid or fluid, exhibit behavior influenced by both displacement and velocity. Devices utilizing viscous fluid dissipation primarily respond to velocity changes

1.2.2.1. Hysteretic devices

The described devices dissipate energy regardless of loading rate and fall into two categories: metallic dampers, which use metal yielding for energy dissipation, and friction dampers, which generate heat through dry sliding friction.

a) Metallic dampers

They are counted among the most effective mechanisms for dissipating input energy to a structure during an earthquake. In traditional metallic structures, seismic design relies on the ductility of framing elements to absorb seismic energy. There are many new designs such the one shown in Figure I.7[8].

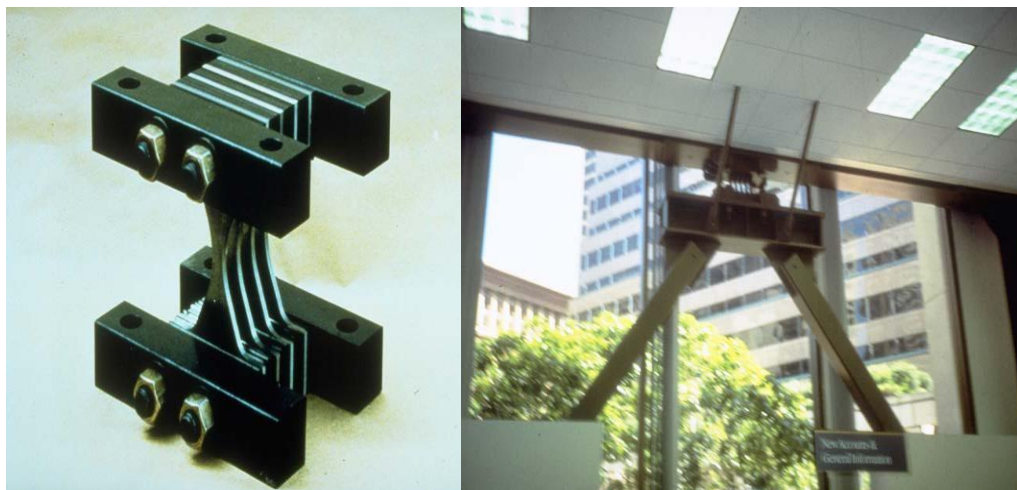


Figure I.7: Metallic damping devices[9]

b) Friction dampers

Friction shock absorbers utilize high-resistance steel rods to fix together a set of plates, creating a friction mechanism that dissipates energy through hysteretic loops in the load-

deformation diagram (Figure I.8). Several types of friction damper have been developed, including[10]

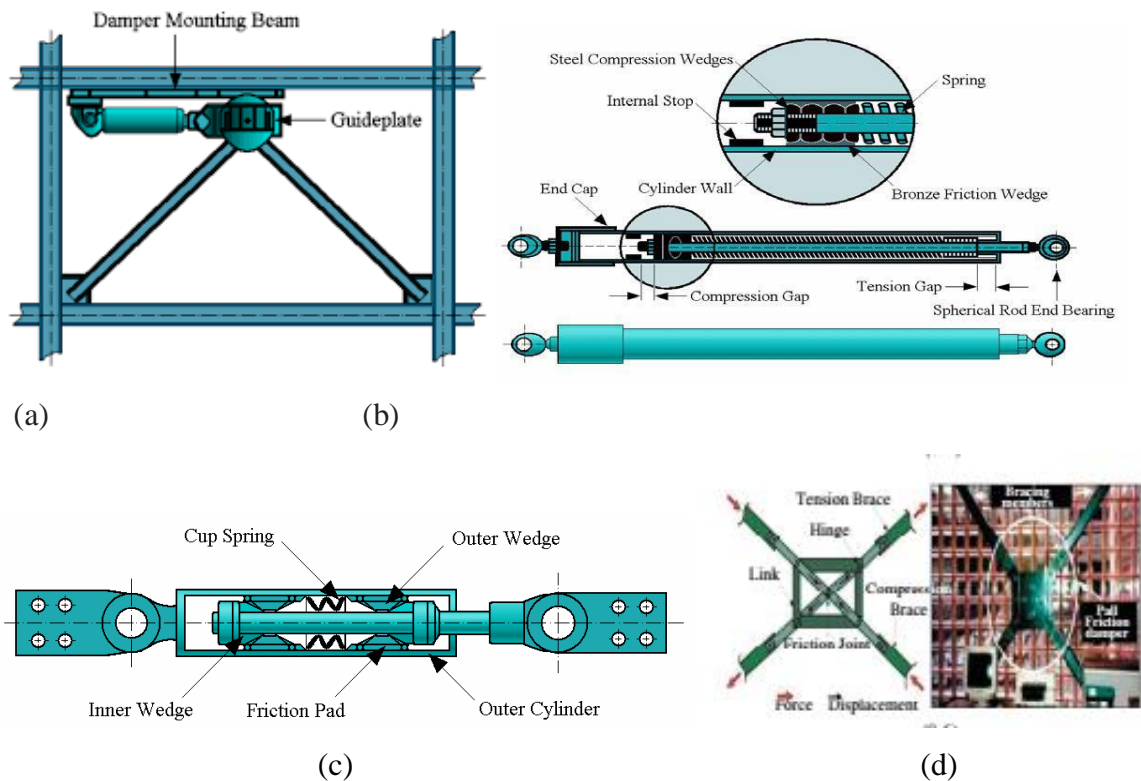


Figure I.8: a) Installation of Sumitomo friction damper in steel frame b)Energy Dissipating Restraint –c)Uniaxial friction damper d)Pall Friction Damper [11]

1.2.2.2. Viscoelastic Shock Absorbers

Viscoelastic dampers (VE) utilize viscoelastic materials with a high damping coefficient to dissipate energy through deformation, often including rubber and/or polymers. These dampers typically comprise layers of viscoelastic material bonded to steel plates, as depicted in Figure I.9[12, 13].

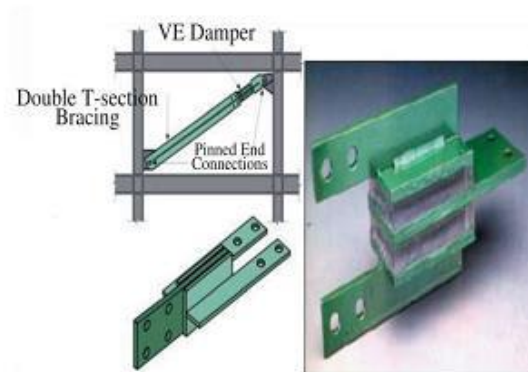


Figure I.9: Typical solid VE damper[14]

1.2.2.3. Viscous fluid shock absorbers

This system is a passive damping mechanism that utilizes shear forces from the motion of a viscous fluid, like hydraulic oil, to convert mechanical energy into heat energy, thereby diminishing vibration amplitudes within a structure. The concept is illustrated in Figure I.10.

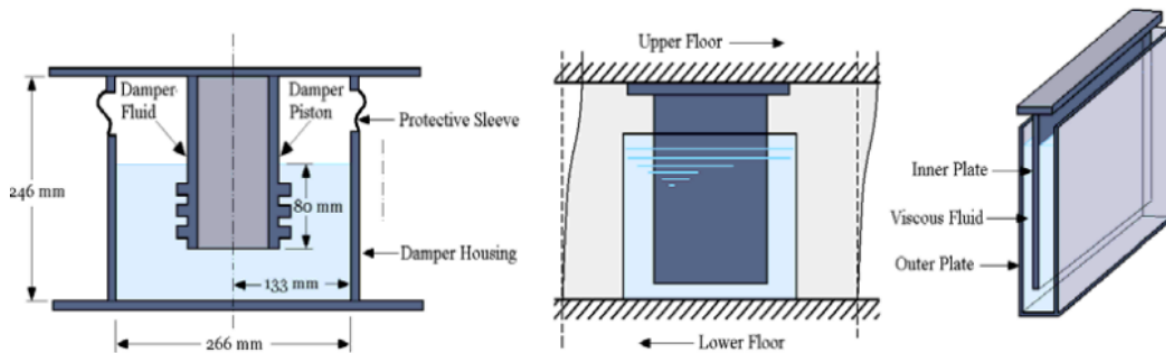


Figure I.10: Cylindrical container fluid damper from GERB [15]

1.2.2.4. Tuned Mass Damper (TMD)

A tuned mass damper usually consists of a mass that is connected to a structure by a spring and a damping element without any other support, in order to reduce vibration of the structure and to regulate vibrations caused by wind in tall buildings, the TMD is usually tuned with respect to the main frequency of the structure. One of the most famous TMDs in the one installed in the Taipei 101 Tower in Taiwan (Figure I.11).

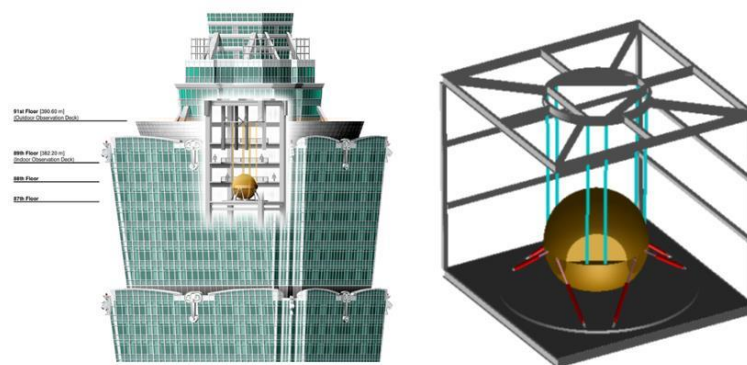


Figure I.11: Pendulum tuned mass damper [16]

1.2.2.5. Tuned Liquid Damper

Tuned liquid dampers are similar to tuned mass dampers except that the mass spring damper system is replaced by the container filled with fluid. To minimize the impact of external forces on the structure, it may employ a variable orifice to achieve optimal damping.

I.3.Active control systems

An active control system is characterized by its reliance on a substantial power source, typically electro-hydraulic or electro-mechanical actuators, to apply control forces to a structure. These control forces are determined through feedback from sensors that measure the structure's excitation and/or response. The primary impact of active control systems is to adjust damping levels with minimal changes to stiffness. The flow diagram of active control systems is depicted in Figure I.12. Examples of active control include the Active Mass Damper and Active Brace System

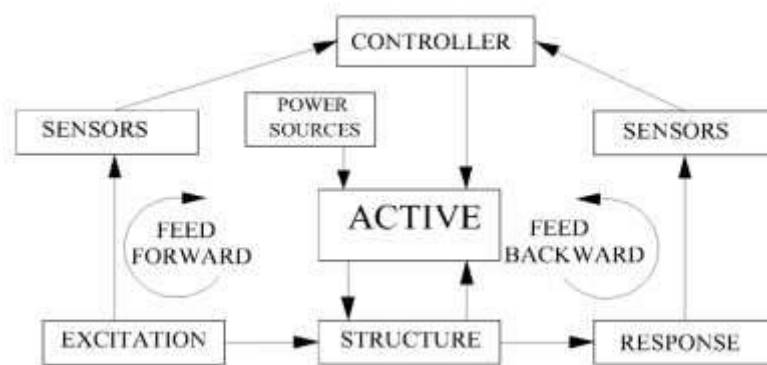
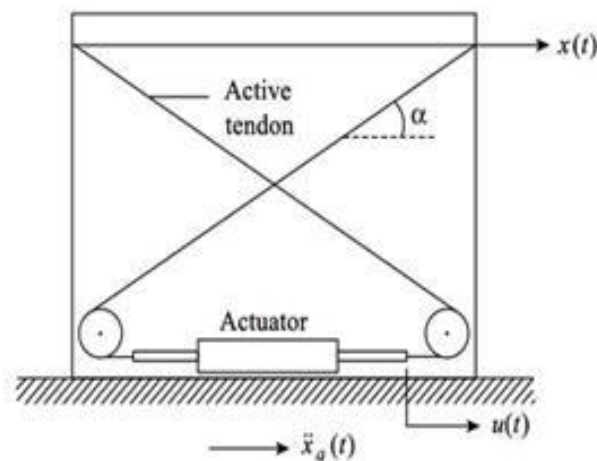


Figure I.12: Active Control System [17]

I.3.1Active Tendon Damper

Active Tendon Control systems consist of a set of pre-stressed tendons whose tension is controlled by electro-hydraulic servo mechanisms. Figure I.13 illustrates a typical configuration of an active control system using active tendons. Active tendons are installed between two floors of a building structure.



FigureI.13:Schematic diagram of active tendon system [16]

I.3.2. Active Brace System

Active Brace Systems comprise solid diagonal tube braces, a hydraulic power supply, and analog/digital sensors. Sensors on the building's foundation and floors measure acceleration, while control system actuators facilitate longitudinal expansion and contraction of the braces. These systems are adaptable to buildings of any height, suitable for retrofitting existing structures or incorporating into new constructions. A schematic illustration is shown in figure I.14.

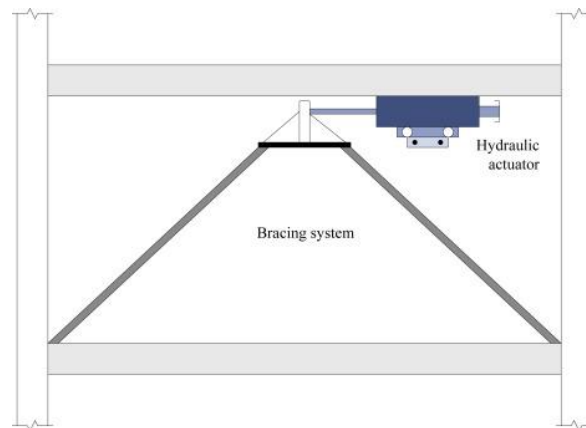


Figure I.14: Active bracing system with hydraulic actuator [18]

I.3.3. Active Mass Damper Systems

Active Mass Damper (AMD) systems utilize actuators installed on structures to regulate their movements, thereby enabling manipulation for improved control system efficiency. An AMD has a similar working principle as a TMD with the only difference of incorporating an actuator to drive the movable mass as it can be seen in Figure I.15.

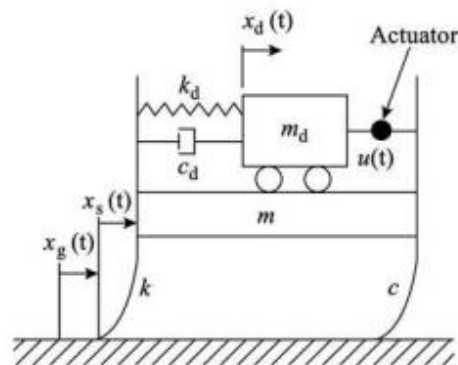


Figure I.15: Schematic Active Mass Damper (AMD) [18]

I.4. Semi-active control systems

A semi-active control system utilizes a small external power source, typically a battery, and relies on the structure's motion to generate adjustable control forces. Sensors provide

feedback on the structure's excitation and response. The feedback can be measured remotely. Semi-active controllers combine features of both active and passive systems, with a schematic diagram shown in Figure I.16. These systems often originate from passive control systems modified to adjust mechanical properties. Similar to active systems, controller processes feedback and generates a command signal, while control forces are developed based on the structure's motion, similar to passive systems. The control forces mainly oppose structural motion, contributing to global stability

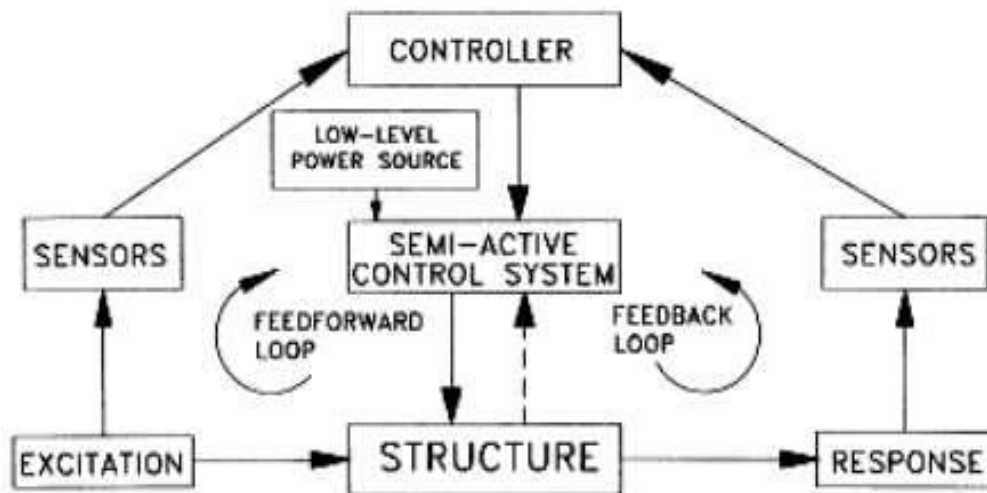


Figure I.16: Semi-Active Control System [17]

1.4.1. Electrorheological Dampers

These devices employ smart electrorheological (ER) fluids—non-conductive viscous fluids with suspended dielectric particles. Under an electrical field, these particles polarize and align, inducing resistance to fluid flow. This allows rapid and reversible changes in flow resistance, controlled by adjusting the applied electrical field. ER dampers, initially proposed by Makris, utilize these smart properties to modulate damping force generation. Illustrated in Figure I.17, the damper comprises a cylinder with a balanced piston rod and piston head. Voltage adjustment alters the electric field, controlling both the ER fluid's behavior and the damper's capacity. Energy dissipation occurs through ER effects from fluid shearing and friction effects from viscous fluid passing through an orifice. However, three limiting factors for ER dampers in large structures are their limited yield stress (around 5-10 kPa), potential applicability issues due to manufacturing impurities, and the high voltages required to control the ER fluid (approximately 4000 V)

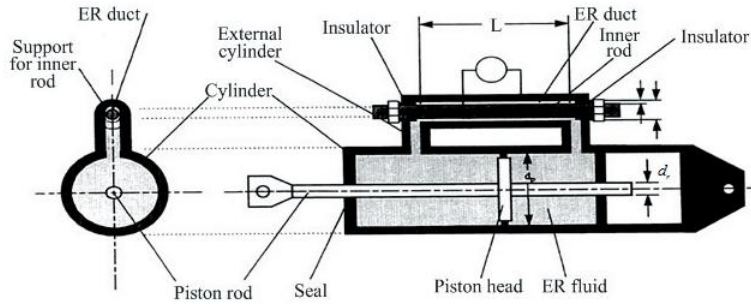


Figure I.17: Schematic of an Electrorheological Fluid Damper [19]

I.4.2. Magnetorheological Dampers

Magnetorheological (MR) fluids, discovered by Jacob Rabinow in the early 1950s[20], are smart materials that alter their fluid properties in the presence of a magnetic field. These fluids, akin to ER fluids, typically consist of micron-sized magnetically polarizable particles dispersed in a viscous fluid like silicone oil. When exposed to a magnetic field, the particles polarize, causing visco-plastic behavior and resistance to flow (see Figure I-18. a). MR fluids can rapidly transition from free-flowing to semi-solid states in milliseconds under a magnetic field, similar to ER fluids responding to electric fields. The control force generated by MR fluids can be adjusted by varying the magnetic field strength. In the depicted system (Figure I-18. b), the magnetic field is applied perpendicular to the fluid flow direction. Advantages of MR fluids over ER fluids include higher yielding strength (approximately 50-100 kPa), stability across a wide temperature range, insensitivity to contaminants resulting in low production costs, and low power requirements (20-50 watts)

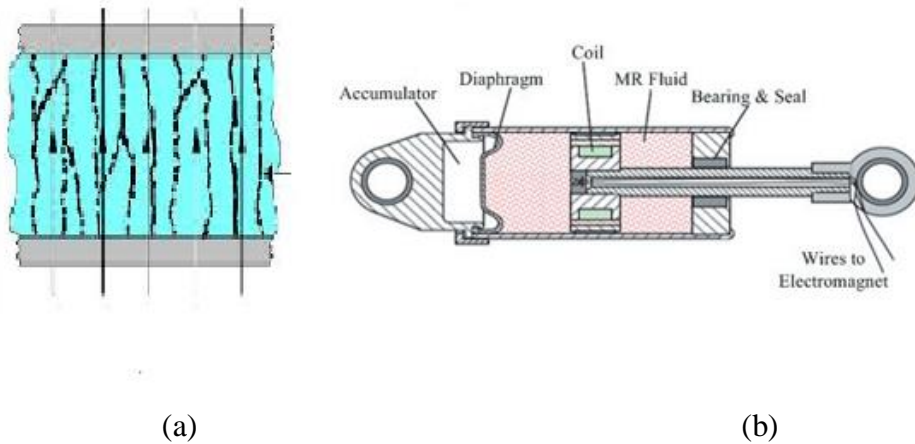


Figure I.18: a) Magnetorheological fluid b) Magnetorheological fluid Damper [19]

I.4.2.1. Rheological models of the MR damper

To simulate the MR damper behavior in a numerical model, a multitude of rheological models were developed and investigated by researchers. The most reliable models are:

a) Bouc-Wen model

The basic Bouc-Wen model comprises three elements arranged in parallel: a spring, a dashpot, and a Bouc-Wen block, as illustrated in Figure I.19.

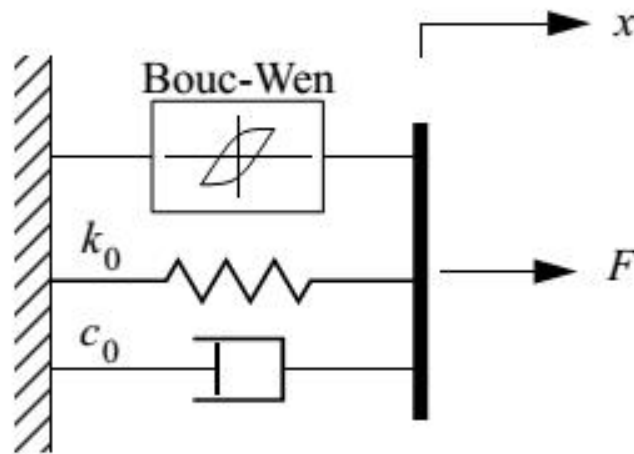


Figure I.19: Simple Bouc-Wen model for MR dampers [21]

Based on the mechanical arrangement depicted in Figure I-18, the damper force is given by:

$$F(t) = c_0 \dot{x} + k_0(x - x_0) + az \quad (I.1)$$

Where c_0 is the viscous coefficient, k_0 the stiffness coefficient and z is an evolutionary variable associated with the Bouc-Wen block and governed by:

$$z = -\gamma |\dot{x}| z |z|^{n-1} - \beta \dot{x} |z|^n + A \dot{x} \quad (I.2)$$

The parameters c_0 , k_0 , α , β , γ , n and A are usually called characteristic or shape parameters of the Bouc-Wen model and are functions of the current, amplitude and frequency of excitation

b) Modified Bouc-Wen model

The modified Bouc-Wen model integrates a simple Bouc-Wen block with two additional mechanical elements, a spring and a dashpot, as depicted in Figure I.20

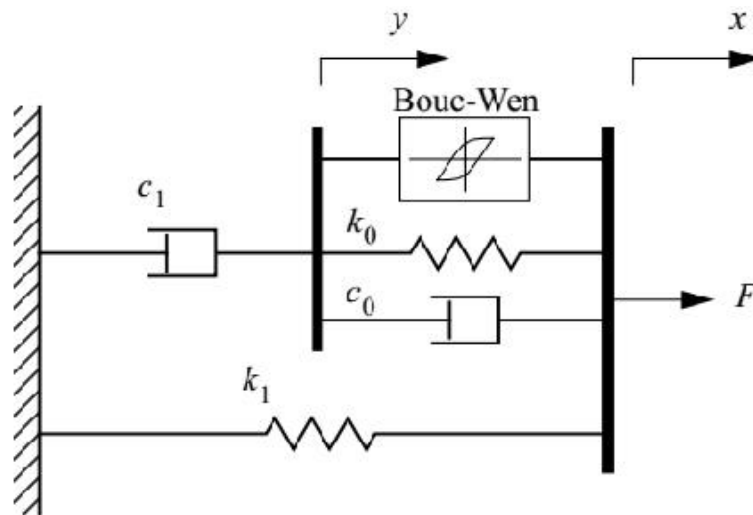


Figure I.20: Modified Bouc-Wen model for MR dampers

In this parametric model, the force exerted by the MR damper can be calculated using the following equations:

$$f_{MR}(t) = c_0(\dot{x} - \dot{y}) + k_0(x - y) + k_1(x - x_0) + az = c_1\dot{y} + k_1(x - x_0) \quad (I.3)$$

where z is the evolutionary variable given by:

$$z = -\gamma|\dot{x} - \dot{y}|z|z|^{n-1} - \beta(\dot{x} - \dot{y})|z|^n + A(\dot{x} - \dot{y}) \quad (I.4)$$

and y is the internal displacement of the MR damper given by:

$$y = \frac{1}{(c_0 - c_1)} [c_0\dot{x} + k_0(x - y) + az] \quad (I.5)$$

In these equations c_0 represents the viscous damping at high velocities c_1 adjusts the damping for the roll-off effect seen at low velocities k_0 controls stiffness at high velocities k_1 is associated with accumulator stiffness, and x_0 incorporates the accumulator effect. Similar to the simple Bouc-Wen model, adjusting parameters A , β , γ and n alters the nonlinear shape of the hysteretic curve. Typically, these parameters remain constant, while α , c_1 , c_0 vary as functions of the applied current.

Since this study involves the usage of a semi-active magnetorheological damper the modified Bouc-Wen model will be adopted in the numerical study.

1.5. Hybrid control systems

Hybrid control systems have been developed to address the drawbacks of active systems and push the limits of passive and semi-active systems. Indeed, hybrid control involves combining techniques from both passive and active control. However, the three types of control passive,

active, and semi-active, can also be used in parallel or in series to leverage the benefits of each type and minimize the impact of their disadvantages when used individually. Hybrid control systems have been considered attractive solutions since 1990. Two typical hybrid systems have been developed: hybrid mass damper, hybrid base isolation system[18]

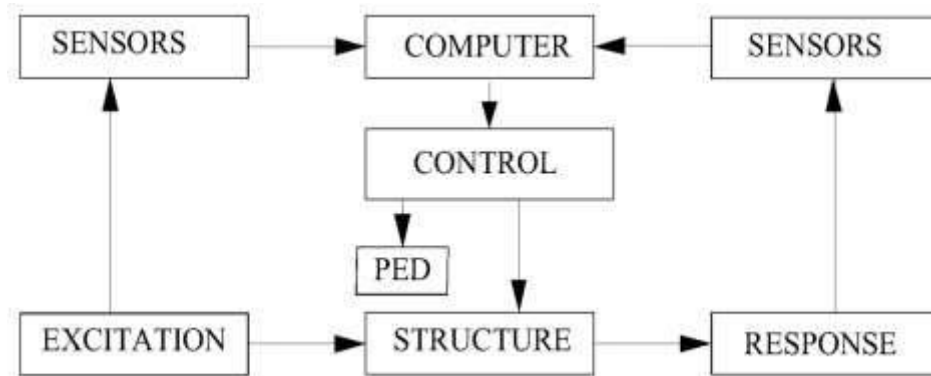


Figure I.21: Hybrid Control Systems[17]

1.5.1. Hybrid Mass Dampers

A Hybrid Mass Damper (HMD) combines either a passive Tuned Mass Damper (TMD) with an active control actuator or an Active Mass Damper (AMD) with a TMD, as depicted in Figure I-22. By connecting an AMD to a TMD rather than the main structure, the mass of the AMD can be significantly reduced to 10-15% of that of the TMD. HMDs require less energy and forces compared to a full AMD system with similar performance, mainly because the AMD in an HMD is designed to enhance control efficiency for the structure's higher modes, while the fundamental mode is controlled by the TMD. This cost-effective feature has led to the widespread adoption of HMDs in full-scale building structures, although their use may be restricted by space limitations.

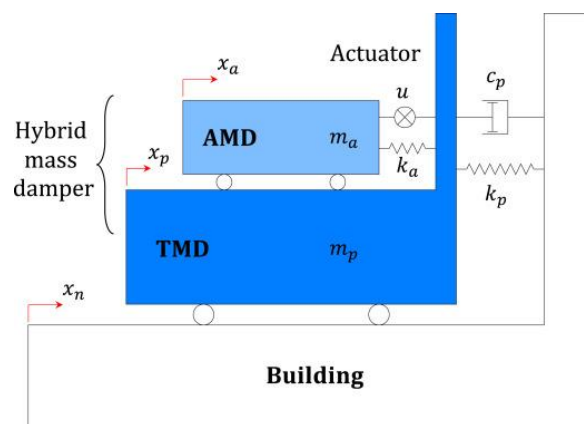


Figure I.22: The schematic diagram of the hybrid mass damper system [18]

1.5.2. Hybrid Base-Isolation System

Hybrid Base-Isolation systems dominate the landscape of hybrid control solutions in the United States. This category can be divided into two types [44]. The first type, proposed by Yoshioka et al. [79] and illustrated in Figure I.23.a employs magnetorheological (MR) fluid dampers on the superstructure instead of the active tendon utilized in the second type. The second type, investigated by Cheng and Jiang [80], incorporates a base isolation unit placed between the foundation and the structure, along with an active tendon control system on the superstructure, as depicted in Figure I.23.b.

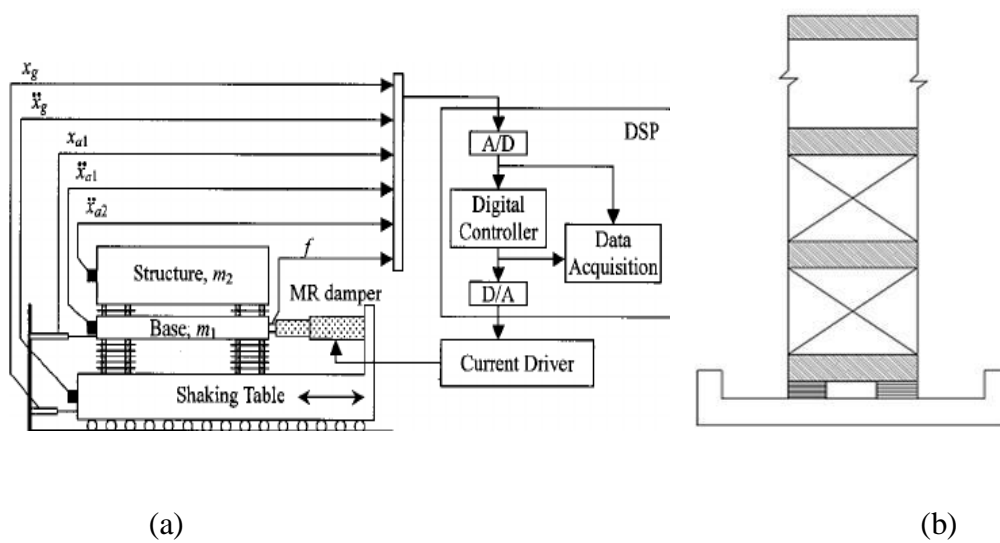


Figure I.23: a) Hybrid Base-Isolation system with MR damper [22] b) Hybrid Base-Isolation system with actuators [19]

I.6. Conclusion

In summary, seismic control systems for buildings, comprising active, passive, hybrid, and semi-active systems, are pivotal in minimizing the effects of earthquakes. Active systems dynamically regulate the building's response in real-time, while passive systems depend on built-in damping mechanisms. Hybrid systems merge these approaches, providing adaptability and strength. Semi-active systems, such as MR dampers, offer adjustable damping characteristics, bolstering structural durability. Each system type presents distinct benefits, fostering safer and more resilient buildings in earthquake-prone areas.

Chapter II: The nonlinear behavior of structures

Chapter II: The nonlinear behavior of structures

II.1. Introduction

During severe ground shakings, structures undergo deformations and transition into a nonlinear, inelastic range of behavior. Specifically, these structures experience oscillatory motion in response to earthquakes, manifesting a hysteresis loop in their force–displacement relationships[23].

II.2. Literature review

In the event of a severe earthquake, structures undergo a transition from their elastic state, rendering linear systems inadequate for accurately depicting their seismic behavior. Hence, nonlinear analysis becomes imperative to properly assess their response. Such analyses require behavior models reflecting the force-displacement relationship, commonly known as hysteretic models, based on loading history. Despite extensive research on structural control systems, those accommodating nonlinear structure behavior remain relatively limited. Notable among these is the algorithm proposed by Cheng and Tian in 1992 [24], tailored for active control systems compatible with nonlinear structures. Shimida *et al.*[25] applied the Instantaneous Optimal Control algorithm to a 5-story nonlinear building with bilinear force-displacement characteristics, while Yang *et al.*[26] explored hybrid control systems for nonlinear structures. Additionally, Yang *et al.*[27] investigated the effectiveness of the Sliding Mode Control algorithm, and later [28], demonstrated the performance of an Optimal Polynomial Control algorithm while considering nonlinear structures.

Further Agrawal introduced an optimal polynomial control approach for linear stochastic systems using stochastic dynamic programming. Later, this control strategy was extended to nonlinear systems in 1996[28]. Building structures subjected to dynamical loadings can undergo various forms of damage, including crack opening, post-yielding and buckling of metallic elements, strength and stiffness degradation, and other localized inelastic behaviors [29].

Developing mathematical models for nonlinear building systems is challenging, especially when integrating highly nonlinear hysteretic actuators or dampers to enhance energy dissipation. Although the building structure is often assumed to be linear, incorporating nonlinear dampers introduces overall system nonlinearity Ramallo *et al.*[30].

Cimellaro *et al.* in 2009 proposed a novel method for designing an equivalent passive control system in nonlinear structures [31]. In another study, they presented an innovative approach for designing nonlinear structures equipped with active control devices. Furthermore, Reinhorn *et al.* in 2009 introduced a unified method for designing passive control systems applicable to both linear and nonlinear structures [32], integrating principles from active control. Lavan and Dargushin in 2009 introduced a multi-objective optimization method for supplemental energy dissipating devices, comparing various systems [33]. Li *et al.* in 2010 introduced the Adaptive Fuzzy Sliding Mode control algorithm to mitigate vibrations in nonlinear structures [34]. More recently, Fabio *et al.* in 2013 evaluated the performance of passive control devices in a nonlinear 6-story structure [35]. Ray *et al.* in 2013 developed nonlinear elastic and inelastic spectra for structures incorporating both inherent and supplemental damping [36].

According to Cimellaro and Reinhorn [37], the performance level of an integrated structure is typically determined by multiple limit states and controlled by multiple failure modes. Additionally, recent studies have indicated that passive control systems are less sensitive to changes in structural properties due to nonlinearity or errors in modeling and estimation [38]. Boccamazzo *et al.* (2020) proposed the earthquake mitigation effect of hysteretic Tuned Mass Dampers for nonlinear structures [39].

II.3. Basic Concepts of Nonlinear Phenomena

To comprehend nonlinearity in material, it's crucial to grasp the concept of linearity first. A linear system denotes that the relationship between input and output is linear. In structural, this means that the relationship between applied loads (input) and displacements (output) is linear—doubling the load results in a proportional doubling of displacement. This relationship can be mathematically described using a linear operator [40]. However, linearity may either accurately represent reality or merely stem from simplifying assumptions made for analytical purposes. In the following, the fundamental assumptions of linear analysis of structures.

- The structures are made of linearly elastic materials, adhering to Hooke's law, where stress is directly proportional to strain.
- The deformations of the structures are so small

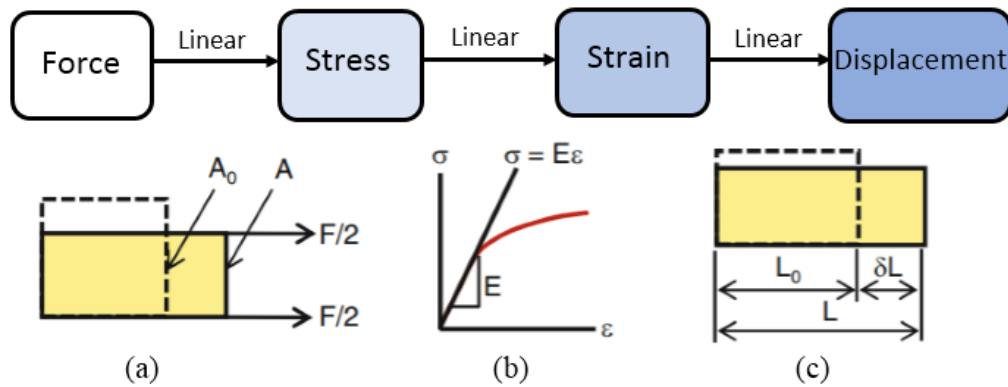


Figure II.1: Linearity in structural systems[41].

Linearized formulations often fall short in explaining many phenomena. Nonlinear analysis aims to enhance the simulation of structural behavior. Nonlinearity means the force versus displacement plot is not a straight line; the structure's stiffness varies with loading. Most structures do not exhibit a linear force-displacement relationship. A structure is considered nonlinear if loading significantly alters its stiffness. Typical reasons for these changes include: Material does not obey Hooke's law, material plastically deforms after the elastic limit, and large deformation due to small or larger loads.

II.3.1. Types of nonlinearities

Nonlinear analysis considers the effects of several factors, such as geometric nonlinearity and material nonlinearity. By incorporating these complexities, engineers can gain insights into the structural response beyond the limitations of linear analysis.

II.3.1.1. Geometric nonlinearity

When a solid's deformation is significant enough that the undeformed and deformed shapes differ substantially, finite deformation occurs. In this state, linear strain-displacement or equilibrium equations based on the undeformed geometry are no longer feasible. Geometric nonlinearities arise from changes in geometry due to load application, impacting the structural response. These nonlinearities typically occur when displacements are large.

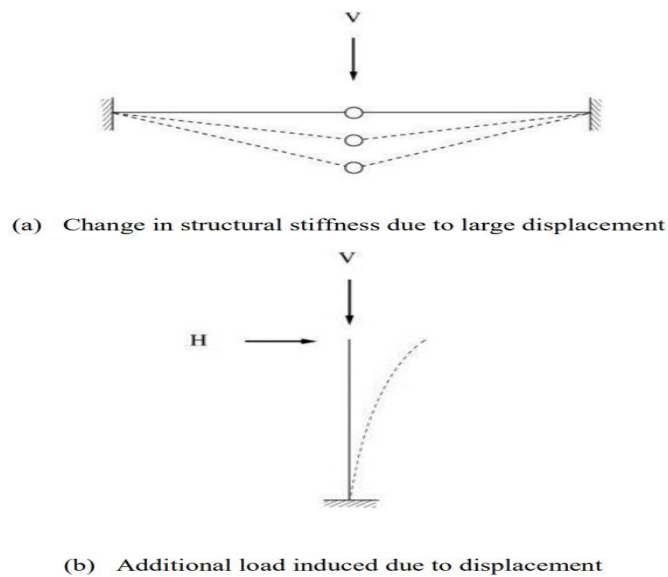


Figure II.2: Structural system requiring geometric nonlinear analyses

II.3.1.2. Material nonlinearity

Material nonlinearity refers to the behavior of materials that do not follow a linear relationship between stress and strain. In linear materials, stress is directly proportional to strain, and the relationship is described by Hooke's Law. However, many materials exhibit nonlinear behavior under certain conditions.

II.4. Inelastic Analysis of Dynamic Response

II.4.1. Inelastic Domain

The elasticity of a material refers to its capacity to return to its original shape after the removal of an applied force, indicating elastic behavior with no permanent deformation. Materials may exhibit linear elasticity, with stress-strain relations depicted as in Figure II.3.a, or nonlinear elasticity, showing curvature as in Figure II.3.b. In both cases, loading and unloading curves coincide. Alternatively, inelastic materials, as shown in Figure II.3.c, do not follow the same unloading path, resulting in permanent deformation.

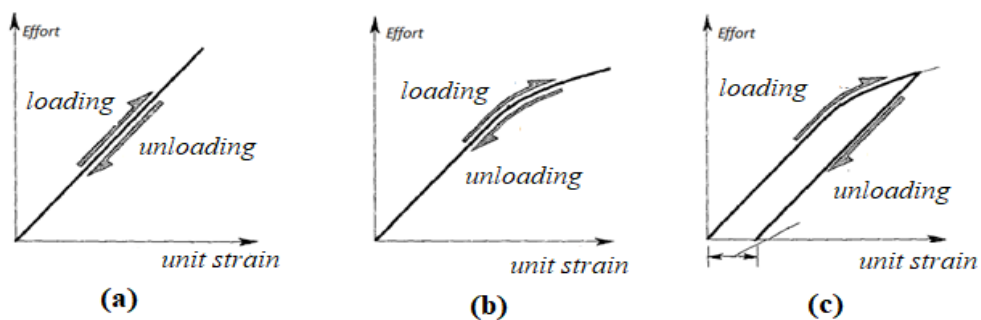


Figure II.3: Material (a) linear elastic, (b) nonlinear elastic and (c) inelastic

II.4.2. Hysteretic Response

Figure II.4 shows a material's loading from 0 to point A, then unloading along trajectory AB. Initially, the material displayed elastic behavior with its initial modulus of elasticity. However, entering the inelastic domain before point A resulted in permanent deformation. Moreover, the energy accumulated up to point A isn't fully released during unloading, leading to energy dissipation represented by the shaded region. In the inelastic domain, only a fraction of the absorbed energy is recovered during unloading.

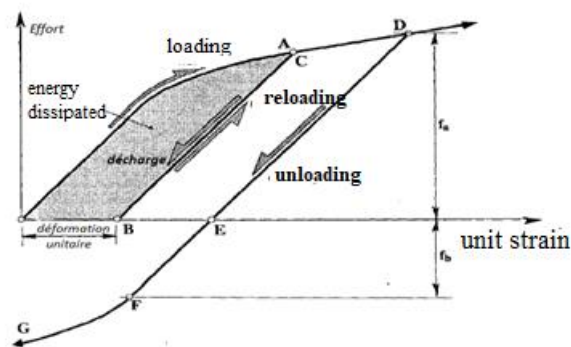


Figure II.4: Effect of loading and unloading with reversal of the direction of effort

When a material experiences repeated loading, unloading, and reloading cycles in opposite directions, surpassing its elastic limit, it exhibits the behavior depicted in Figure II.5, known as hysteresis response.

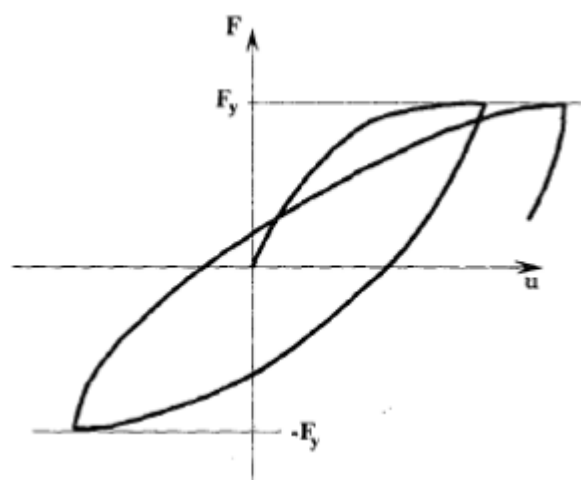


Figure II.5: Force-strain curve for an inelastic material

Hysteresis is a system property wherein it tends to retain a specific state even after the external cause ceases. It describes the behavior of structural materials when experiencing deformations or alternating stresses beyond the linear or elastic response range.

II.4.3. Mathematical Model of Hysteresis

The elastoplastic model depicted in Figure II.6.a is mainly included for educational purposes because of its simplicity, making it usable even for manual calculations. The Ramberg-Osgood model depicted in Figure II.6.b has been recognized for decades as suitable for describing hysteresis in various types of steel structural elements. Meanwhile, the degrading stiffness model shown in Figure II.6.c is applied to describe numerous instances involving reinforced concrete and structural masonry.

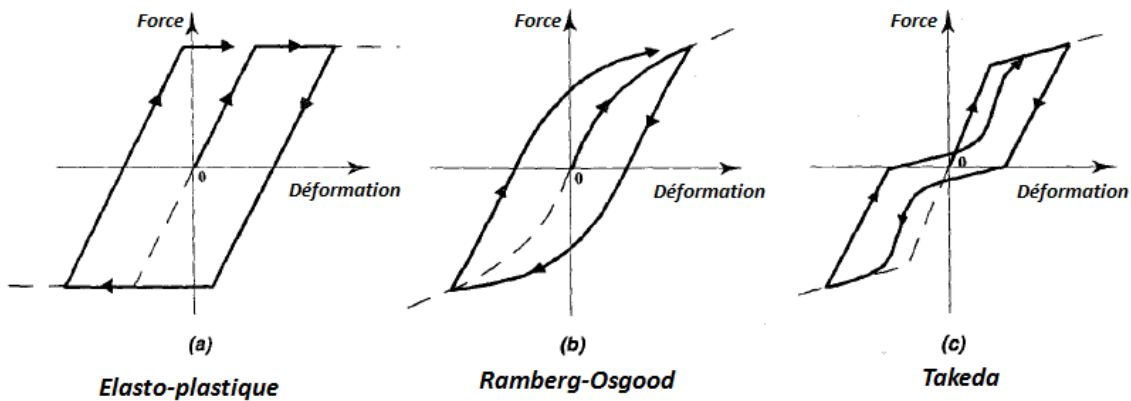


Figure II.6: Model of Hysteresis

II.4.3.1. Elasto-plastic Model

The elastoplastic model, depicted in figure II.7, simplifies the description of force-displacement hysteresis curves. It offers a straightforward mathematical representation by substituting the term $k u$ in dynamic equilibrium equations with the actual force exerted by the spring. This adjustment accounts for inelastic deformations, decoupling the force from direct dependence on the system's deformation u

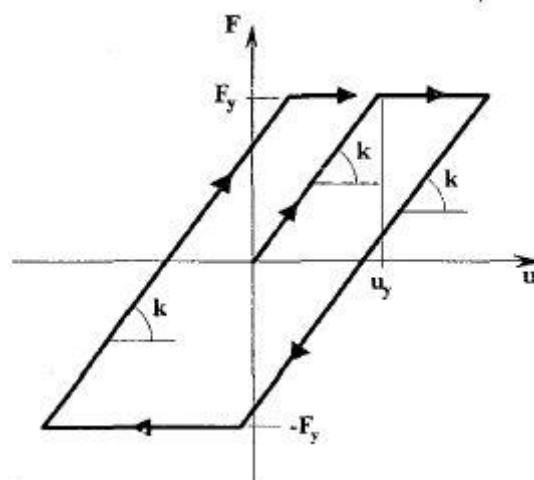


Figure II.7: Force-strain curve for an elastoplastic material

In the elastoplastic model, the material behaves elastically until reaching the elastic limit F_y . Beyond this point, deformation occurs without increased effort. Upon reversing motion, the material returns to elastic behavior until reaching the yield limit on the opposite side, $-F_y$. Deformation energy accumulation is represented by the loading curve area (Figure II.8. a), while during unloading, this energy transforms into kinetic energy, represented by the unloading curve area (Figure II.8.b). The difference between these areas indicates energy dissipation, which converts into heat or other forms (Figure II-8.c)

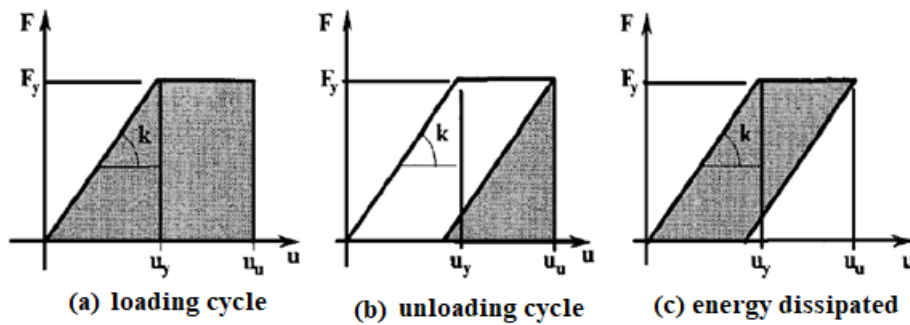


Figure II.8: Energy dissipation in an elastoplastic system

II.5. Mathematical formulation of the material nonlinearity of structures using Bouc-Wen model

One of the most accurate models for describing the material nonlinearity of a structure is the model developed by Bouc and Wen and named after his developers as Bouc-Wen model [21, 42]. This model considers the material nonlinearity by introducing a hysteresis restoring force acting on a nonlinear structure, this hysteresis restoring force is divided into two parts namely; a linear part where the restoring force is linearly proportional to the stiffness of the structure and its displacement and nonlinear part related to a dimensionless variable denoted $\sigma(t)$.

$$f(x(t), \sigma(t)) = \alpha kx(t) + (1 - \alpha)kD_y\sigma(t) \tag{II.1}$$

As it can be seen from equation (II.1), the nonlinear restoring force $f(x(t), \sigma(t))$ is composed of two terms: a linear elastic part represented by the first term $\alpha kx(t)$ and a hysteresis component represented by the second term $(1 - \alpha)kD_y\sigma(t) = f_c(\sigma(t))$. In Equation (II.1) α represents the post-to-pre yield stiffness ratio, k is the stiffness at the elastic limit, D is the yield displacement and $\sigma(t)$ is the dimensionless internal variable introduced to describe the hysteresis component of the deformation. The function $\sigma(t)$ is related to $x(t)$ through the following first-order nonlinear differential equation:

Chapter II: The nonlinear behavior of structures

$$\dot{\sigma}(t) = D^{-1}[A\dot{x}(t) - \beta|\dot{x}(t)||\sigma(t)|^{n-1}\sigma(t) - \gamma\dot{x}(t)|\sigma(t)|^n] \quad (\text{II.2})$$

A, β and γ are dimensionless parameters that govern the shape of the restoring force and the scale of the hysteresis loop, while the smoothness of the force-deformation curve is determined by the parameter n . Figure II.9 explains the working principle of the Bouc-Wen model through graphical illustration.

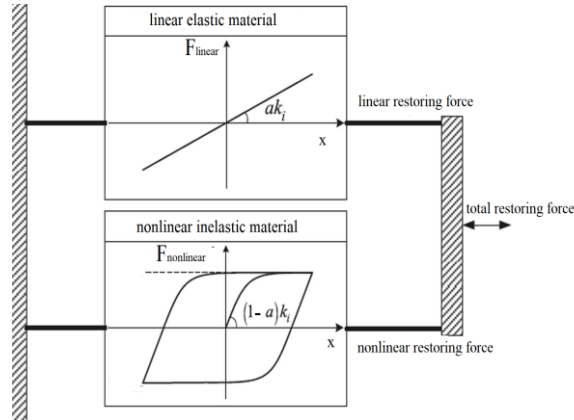


Figure II.9: Bouc-Wen model principle of functioning [43]

The following figure shows how various parameters govern the shape of the hysteresis loop.

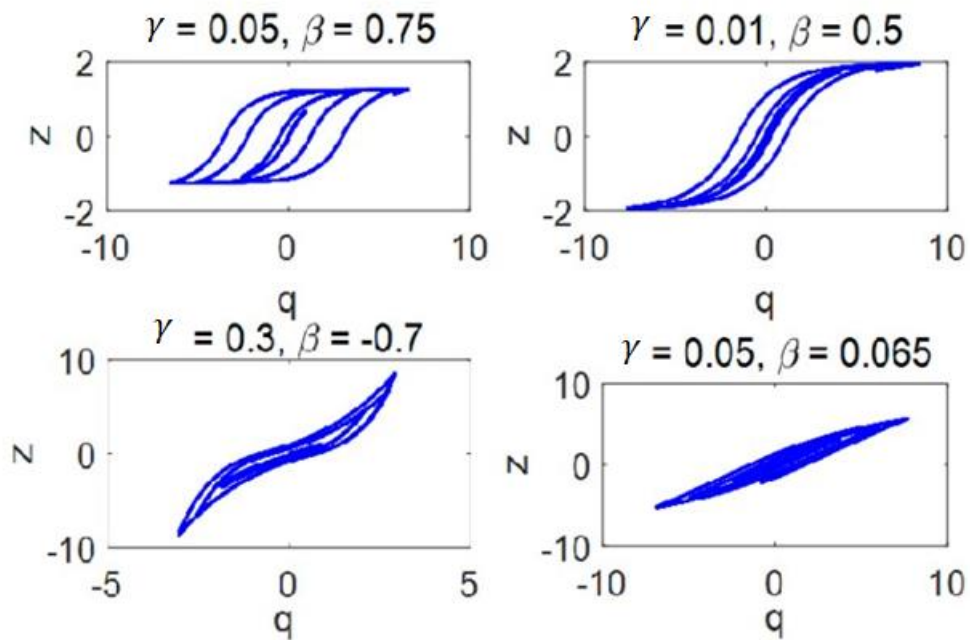


Figure II.10: Various hysteresis loop shapes obtained under different parameters[44].

It is clear from Figure II.10, the Bouc-Wen model can represent various material behavior such as steel structures, reinforced concrete structures and even lead rubber bearing devices [43]. With this in the background the Bouc-Wen model will be used in this study to represent the nonlinear behavior of structures.

II.6. Conclusion

in conclusion, researchers studying seismic events recognize the substantial importance of understanding the nonlinear material behavior of buildings. Mastery of the equations and mathematical concepts related to this behavior is essential for precise prediction and effective mitigation of earthquake effects on structures. By delving deeply into the complexities of nonlinear material response, researchers can devise enhanced seismic design strategies, thus bolstering buildings' resilience against seismic forces. From the literature review it appears that the simplest yet more efficient way to represent nonlinear behavior is the hysteresis Bouc-Wen model that can be used to estimate nonlinear hysteresis force. This model will be used in this study to represent the nonlinear behavior of a multi-degrees of freedom structure.

Chapter III:

Mathematical modeling

Chapter III: Mathematical modeling

III.1. Introduction

Formulating mathematical equations to describe the behavior of a dynamically controlled nonlinear building using semi-active device results in intricate differential equations, the analytical solution of which poses challenges due to their complexity. In our research, we will employ transfer formulation relying on state-space representation to convert n -order differential equations into a system of n first-order differential equations.

III.2. Assumptions and Limitations

In the mathematical formulation for modeling nonlinear buildings equipped with control devices, certain assumptions are made:

- The structure is modeled as a nonlinear system with multiple degrees of freedom, where mass is concentrated at each level with a specified effective stiffness.
- The nonlinearity of the structure is represented through a hysteresis force related to relative velocity of each floor and applied to each floor through a Bouc-Wen hysteresis model.
- The structure is assumed to remain in the elastic zone during seismic excitation, if the relative displacement does not exceed the yielding point.
- The spatial variation of ground motion and any effects due to soil-structure interaction are neglected.
- The structure is subjected to a unidirectional horizontal component of the earthquake.
- The structure's mass is fixed at each floor level, and the floors are considered infinitely rigid in their plane.
- The study is conducted according to the perpendicular plane of the 2D reading, simplifying the problem into a two-dimensional analysis.
- Ground motion is assumed to occur in the direction of the symmetrical planes of the structures.

III.3. Mathematical Model and Equations of Motion

III.3.1. Linear system with a single degree of freedom

A linear system with a single degree of freedom (SDOF) dynamic system is subjected to base acceleration $\ddot{x}_g(t)$, as illustrated in Figure III-1. The structural configuration is a 2D frame modeled as a shear frame building. The primary linear structure is represented by a linear spring with stiffness k , a mass m , and a viscous damper with a damping coefficient c .

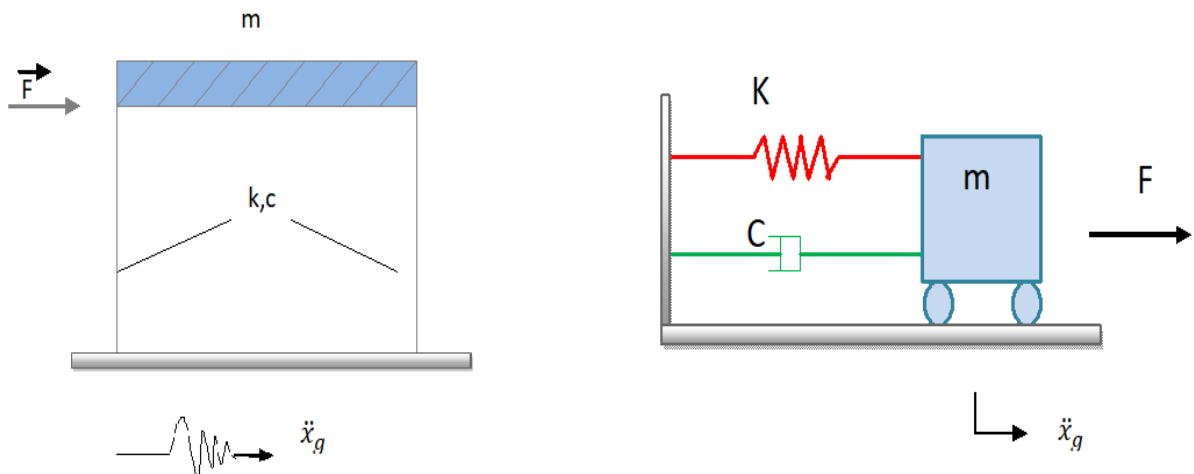


Figure III.1: Equivalent system of Linear system with a single degree of freedom

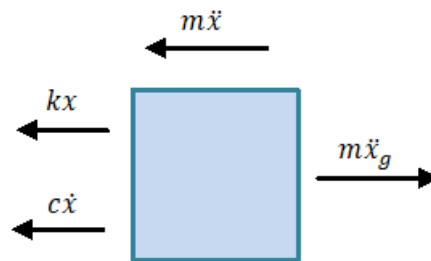


Figure III.2: Free body diagram of Linear system with a single degree of freedom

Based on the free body diagram shown in Figure III.2 the motion equation of the SDOF nonlinear structure can be written as follow:

$$m\ddot{x} + c\dot{x} + kx = m\ddot{x}_g \tag{III.1}$$

III.3.2. Nonlinear system with a single degree of freedom

To represent a nonlinear structure, the same share frame used for the linear model is represented. However, in this case the nonlinear behavior is ensure via a nonlinear element that represents the hysteresis restoring force component based on the Bouc-Wen model detained in Chapter II this later is denoted f_c . Simultaneously, the elastic spring representing the stiffness of the structure is multiplied by a reduction coefficient denoted α .

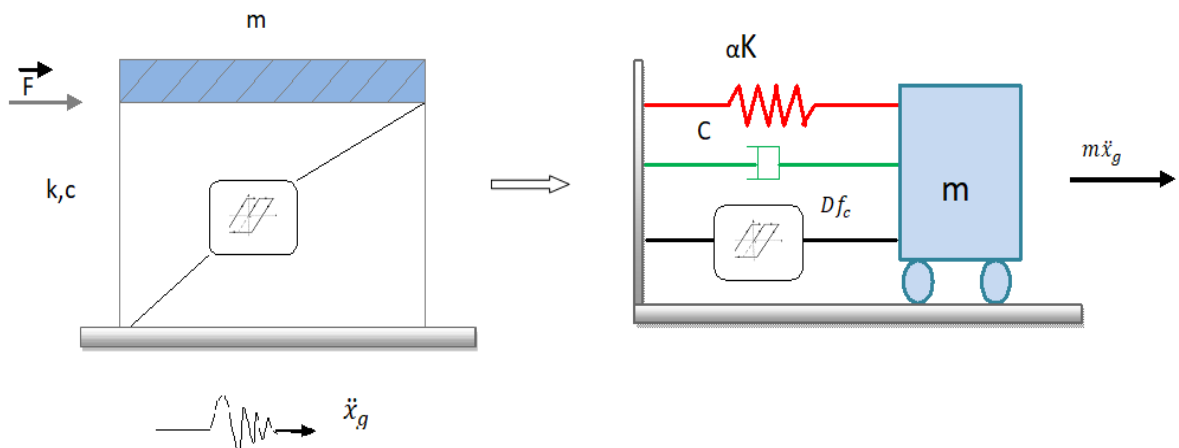


Figure III.3: Equivalent system of linear system with a single degree of freedom

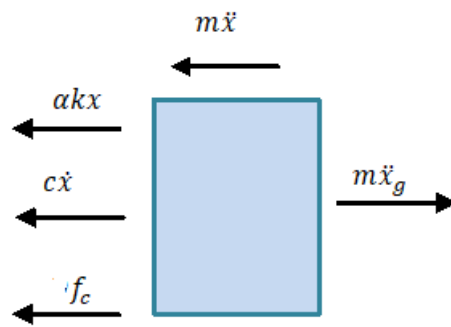


Figure III.4: Free body diagram of -linear system with a single degree of freedom

Based on the free body diagram shown in Figure III.4 the motion equation of the SDOF nonlinear structure can be written as follow:

$$m\ddot{x} + c\dot{x} + \alpha kx + f_c = m\ddot{x}_g \text{ (III.2)}$$

$$m\ddot{x} + c\dot{x} + \alpha kx = m\ddot{x}_g - f_c \text{ (III.3)}$$

III.3.3. Nonlinear system with a single degree of freedom with control device

To represent a nonlinear structure equipped with a MR damper, the nonlinear structure detailed in the previous example is equipped with a MR damper. The MR damper will produce a control force that aims at reducing the response of the structure this later is denoted f_{MR} . The MR damper is governed by the equations detailed in Chapter I.

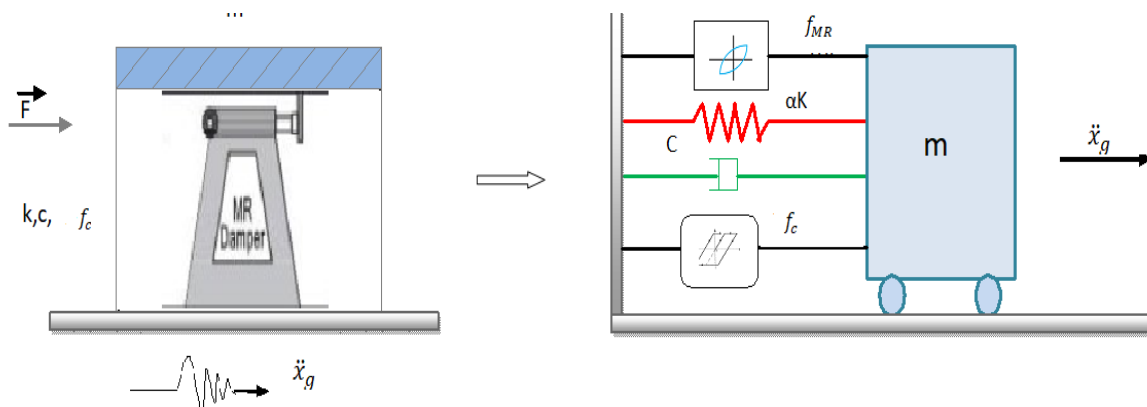


Figure III.5: Equivalent system of Nonlinear system with a single degree of freedom with control device

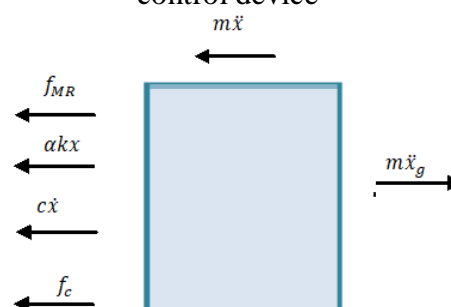


Figure III.6: Free body diagram of Nonlinear system with a single degree of freedom with control device

Chapter III: Mathematical modeling

Based on the free body diagram shown in Figure III.6 the motion equation of the SDOF nonlinear structure equipped with a MR damper can be written as follow:

$$m\ddot{x} + c\dot{x} + \alpha kx + f_c + f_{MR} = m\ddot{x}_g \quad (\text{III.4})$$

$$m\ddot{x} + c\dot{x} + \alpha kx = m\ddot{x}_g - f_c - f_{MR} \quad (\text{III.5})$$

III.3.4. Nonlinear system with multiple degrees of freedom with control device

To assess the behavior of a multi-degrees of freedom nonlinear structure equipped with MR dampers, a multi-floor building is modelled as a shear frame as shown in Figure III.7. The frame is equipped with two MR dampers one located at the first floor and the second one located at the last floor. All the floors express nonlinear behavior through a restoring force denoted f_{Ci} where the subscript i denotes the floor number varying for 1 to n , n being the last floor. The equivalent system of the modelled structure is shown in Figure III.8.

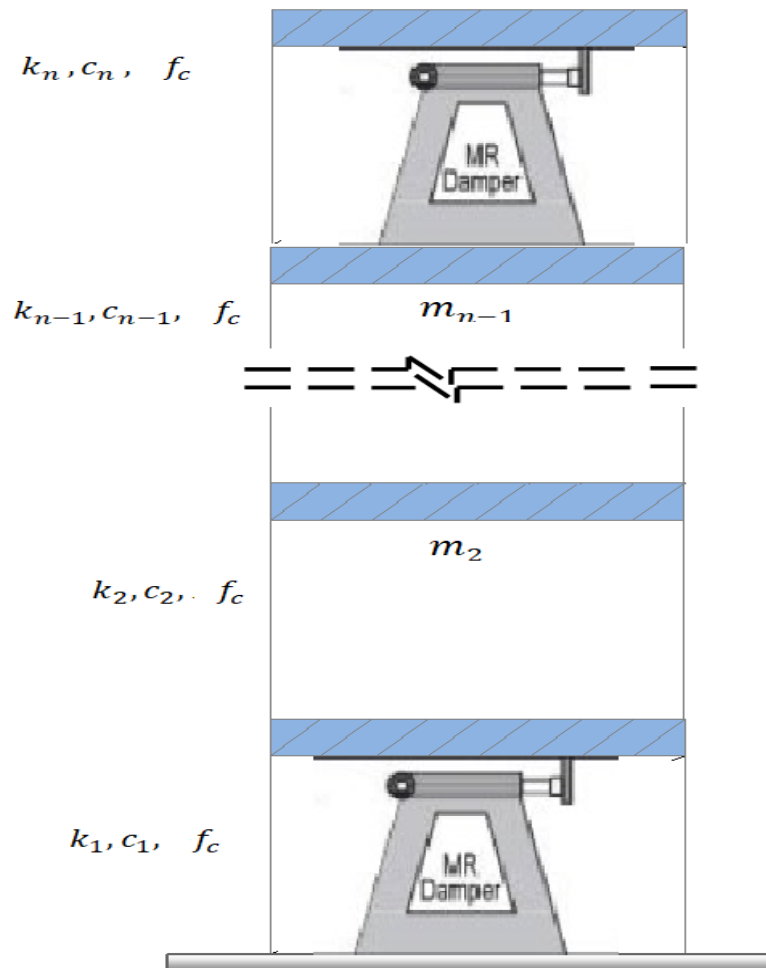


Figure III.7: Nonlinear shear frame structure equipped with MR dampers

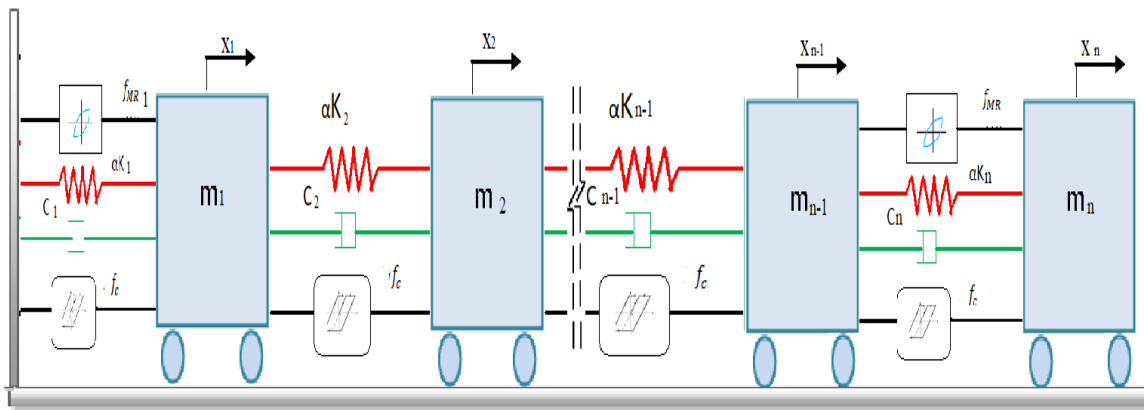


Figure III.8: Equivalent system of Nonlinear system with multiple degrees of freedom with control device located at first and last floors

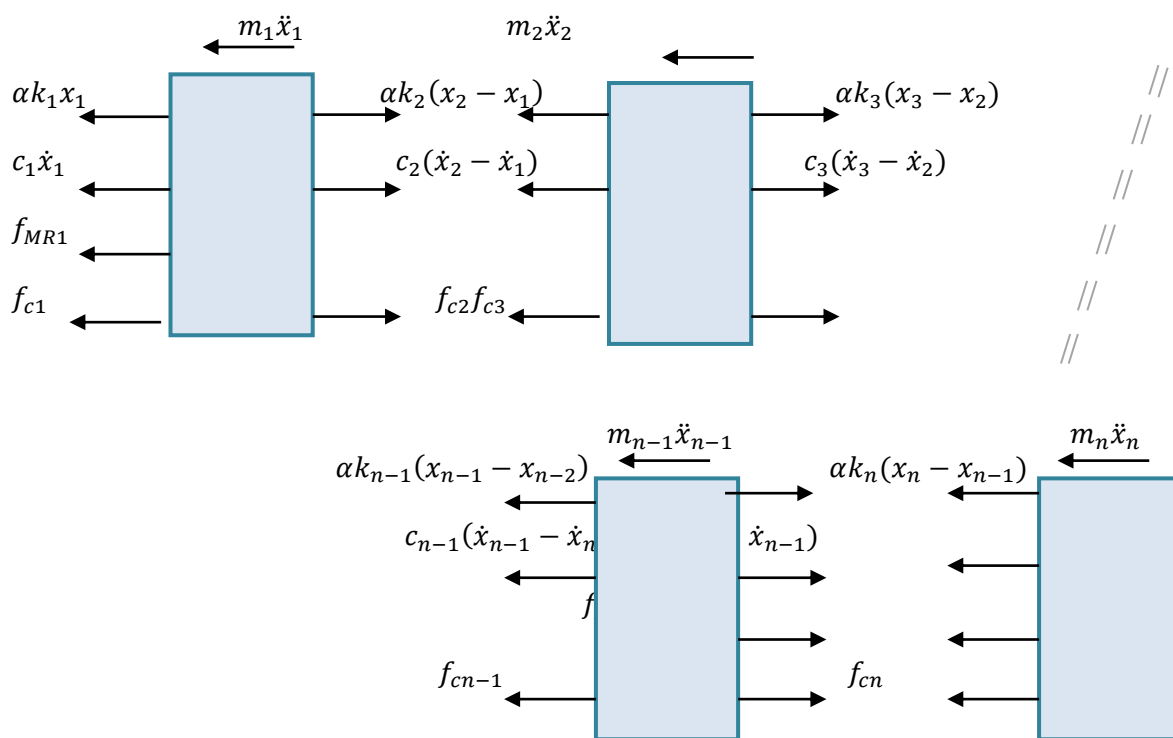


Figure III.9: Free body diagram of Nonlinear system with multiple degrees of freedom with control device

Based on the free body diagram shown in Figure III.9 the motion equation of the MDOF nonlinear structure equipped with a MR damper can be written as follow:

$$\begin{cases} m_1 \ddot{x}_1 + \alpha k_1 x_1 + c_1 \dot{x}_1 + f_{MR1} + f_{c1} - \alpha k_2 (x_2 - x_1) - c_2 (\dot{x}_2 - \dot{x}_1) - f_{c2} = m_1 \ddot{x}_g \\ m_2 \ddot{x}_2 + \alpha k_2 (x_2 - x_1) + c_2 (\dot{x}_2 - \dot{x}_1) + f_{c2} - \alpha k_3 (x_3 - x_2) - c_3 (\dot{x}_3 - \dot{x}_2) - f_{c3} = m_2 \ddot{x}_g \\ \vdots \\ m_{n-1} \ddot{x}_{n-1} + \alpha k_{n-1} (x_{n-1} - x_{n-2}) + c_{n-1} (\dot{x}_{n-1} - \dot{x}_{n-2}) + f_{c_{n-1}} - \alpha k_n (x_n - x_{n-1}) - c_n (\dot{x}_n - \dot{x}_{n-1}) - f_{MR(n)} - f_{c_n} = m_{n-1} \ddot{x}_g \\ m_n \ddot{x}_n + \alpha k_n (x_n - x_{n-1}) + c_n (\dot{x}_n - \dot{x}_{n-1}) + f_{MRn} + f_{c_n} = m_n \ddot{x}_g \end{cases}$$

(III.6)

The n equations of motion of the system shown in Equation III.6 can be written in matrix form as:

$$\begin{aligned}
 & \begin{bmatrix} m_1 & 0 & 0 & \dots & 0 & 0 & 0 \\ 0 & m_2 & 0 & \dots & 0 & 0 & 0 \\ & & & \ddots & & & \\ & & & & & & \\ & & & & & & \\ & & & & & & \\ 0 & 0 & 0 & \dots & 0 & m_{n-1} & 0 \\ 0 & 0 & 0 & \dots & 0 & 0 & m_n \end{bmatrix} \begin{Bmatrix} \ddot{x}_1 \\ \ddot{x}_2 \\ \vdots \\ \vdots \\ \vdots \\ \ddot{x}_{n-1} \\ \ddot{x}_n \end{Bmatrix} + \\
 & \begin{bmatrix} c_1 + c_2 - c_2 & 0 & \dots & 0 & 0 & 0 \\ -c_1 c_2 + c_3 - c_3 & \dots & 0 & 0 & 0 \\ & & \ddots & & & \\ & & & \ddots & & \\ & & & & & \\ & & & & & \\ 0 & 0 & 0 & \dots & c_{n-2} c_{n-1} + c_n c_n & 0 \\ 0 & 0 & 0 & \dots & 0 & -c_n c_n \end{bmatrix} \begin{Bmatrix} \dot{x}_1 \\ \dot{x}_2 \\ \vdots \\ \vdots \\ \vdots \\ \dot{x}_{n-1} \\ \dot{x}_n \end{Bmatrix} + \\
 & \alpha \begin{bmatrix} k_1 + k_2 - k_2 & 0 & \dots & 0 & 0 & 0 \\ -k_1 k_2 + k_3 - k_3 & \dots & 0 & 0 & 0 \\ & & \ddots & & & \\ & & & \ddots & & \\ & & & & & \\ & & & & & \\ 0 & 0 & 0 & \dots & k_{n-2} k_{n-1} + k_n k_n & 0 \\ 0 & 0 & 0 & \dots & 0 & -k_n k_n \end{bmatrix} \begin{Bmatrix} x_1 \\ x_2 \\ \vdots \\ \vdots \\ \vdots \\ x_{n-1} \\ x_n \end{Bmatrix} + \\
 & + [W]\{f_{MR}\} + [H]\{f_c\} = \begin{bmatrix} m_1 & 0 & 0 & \dots & 0 & 0 & 0 \\ 0 & m_2 & 0 & \dots & 0 & 0 & 0 \\ & & & \ddots & & & \\ & & & & & & \\ & & & & & & \\ & & & & & & \\ 0 & 0 & 0 & \dots & 0 & m_{n-1} & 0 \\ 0 & 0 & 0 & \dots & 0 & 0 & m_n \end{bmatrix} \{r\} \ddot{x}_g \quad (III.7)
 \end{aligned}$$

Where:

$[W]$ and $[H]$ are the MR damper location matrix and the hysteresis restoring force distribution matrix, respectively. The number of columns in the $[W]$ matrix will be equal to the number of dampers placed in the structure, while the number of columns in the $[H]$ matrix will be always equal to the number of DOFs since all floors are modelled as nonlinear. $[W]$ and $[H]$ can be detailed as follow:

$$[W]\{f_{MR}\} = \begin{bmatrix} 1 & 0 & \dots & 0 & 0 \\ 0 & 0 & \dots & 0 & 0 \\ \vdots & \vdots & \ddots & \vdots & \vdots \\ 0 & 0 & \dots & 0 & -1 \\ 0 & 0 & \dots & 0 & 1 \end{bmatrix} \begin{Bmatrix} f_{MR1} \\ f_{MR2} \\ \vdots \\ f_{MR(n-1)} \\ f_{MRn} \end{Bmatrix}, \quad [H]\{f_c\} = \begin{bmatrix} 1 & -1 & \dots & 0 & 0 \\ 0 & 1 & \dots & 0 & 0 \\ \vdots & \vdots & \ddots & \vdots & \vdots \\ 0 & 0 & \dots & 1 & -1 \\ 0 & 0 & \dots & 0 & 1 \end{bmatrix} \begin{Bmatrix} f_{c1} \\ f_{c2} \\ \vdots \\ f_{c(n-1)} \\ f_{cn} \end{Bmatrix}$$

$\{r\}$ represents the earthquake distribution vector which is equal to unity vector.

In a compact format the equation (III.7) can be rewritten as follow:

$$[M]\{\ddot{x}(t)\} + [C]\{\dot{x}(t)\} + \alpha[K]\{x(t)\} + [W]\{f_{MR}\} + [H]\{f_c\} = [M]\{r\}\ddot{x}_g(t) \quad (III.8)$$

Where $[M]$, $[C]$ and $[K]$ are the mass, damping, and stiffness matrices, respectively.

$\{x\}$: represents the displacement response vector, a dot represents the first derivative which is the velocity and a double dot represents the second derivative which is the acceleration.

$\{f_c\}$: denotes the nonlinear hysteresis restoring force.

$\{f_{MR}\}$: denotes the damper force.

$\ddot{x}_g(t)$: represents the ground acceleration at each instant of time (t)

$$[M]\{\ddot{x}(t)\} = -[C]\{\dot{x}(t)\} - [K]\{x(t)\} - [W]\{f_{MR}\} - [H]\{f_c\} + [M][r]\{\ddot{x}_g(t)\} \quad (III.9)$$

$$\frac{[M]}{[M]}\{\ddot{x}(t)\} = -\frac{[C]}{[M]}\{\dot{x}(t)\} - \frac{[K]}{[M]}\{x(t)\} - \frac{[W]}{[M]}\{f_{MR}\} - \frac{[H]}{[M]}\{f_c\} + \frac{[M]}{[M]}\{r\}\{\ddot{x}_g(t)\}$$

$$\{\ddot{x}(t)\} = -[M]^{-1}[C]\{\dot{x}(t)\} - [M]^{-1}[K]\{x(t)\} - [M]^{-1}[W]\{f_{MR}\} - [M]^{-1}[H]\{f_c\} + [r]\{\ddot{x}_g(t)\}$$

III.4. System Resolution using State Representation (State Space)

Several numerical techniques exist for solving the equations of motion and modeling the system's behavior over time. Among these methods is the state space representation. A state space model offers a distinct viewpoint on the input-output correlation, contrasting with the transfer function or frequency response function methodologies. This modeling approach emerged in the 1960s to accommodate the growing demand for analyzing large-scale dynamic systems via computers.

The state space model hinges on the notion of state, a concept present in classical dynamics but adapted differently for the state space model[45].

It's a numerical solution method for problems with multiple degrees of freedom (MDOF) of higher order. This method is based on reducing the order of dynamic equations as follows:

If a differential equation is of the 2nd order, it is written as two (2) first-order differential equations. In general, a differential equation of the n^{th} order is transformed into n first-order

Chapter III: Mathematical modeling

equations (thus, the order of the differential equations becomes the number of first-order differential equations)[46].

In state representation, the equations of motion are written as follows:

$$\begin{cases} \dot{z}(t) = Az(t) + Bu(t) \\ y(t) = C_c z(t) + Du(t) \end{cases} \quad (\text{III.9})$$

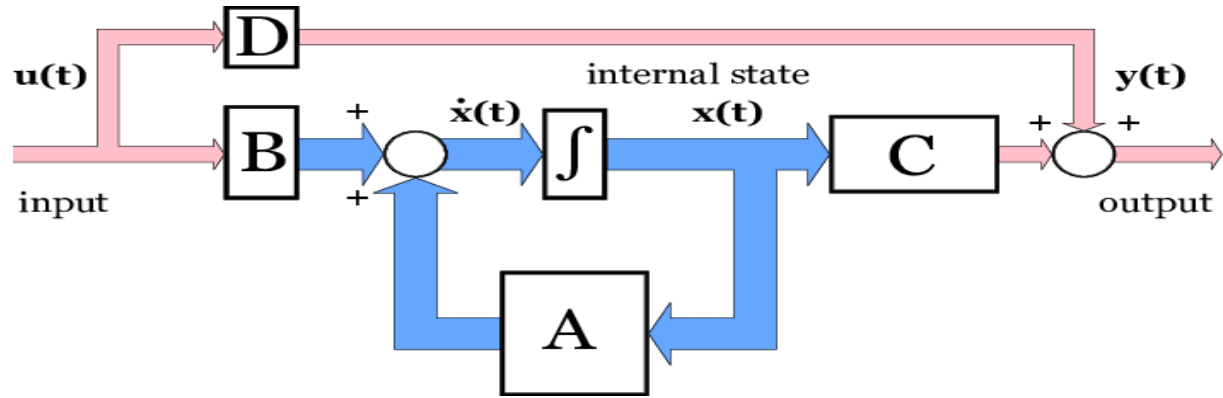


Figure III.10; Block-diagram representation of a state-space model

The state space representation formulation considers four matrices $[A]$, $[B]$, $[C_c]$ and $[D]$ [47]

$[A]$: state matrix $2n \times 2n$, it depends on the parameters of the dynamic system (M, K, C), link between x and \dot{x}

$[B]$: input matrix $2n \times r$ it depends on the inputs (any external (damper) or internal (hysteresis forces acting on the dynamic system) it is directly linked to the internal response and external input.

$[C_c]$: output matrix $2n \times 2n$, depends on the selection of the studied output variable (e.g. displacement/velocity of the primary system)

$[D]$: represents the matrix of direct transmission between the system's inputs and outputs. In the context of dynamics problems, this matrix is typically zero.

To obtain the state-space form shown in Equation (III.9), the motion equation shown in (III.8) is rearranged such as:

$$[M]\{\ddot{x}(t)\} = -[C]\{\dot{x}(t)\} - [K]\{x(t)\} - [W]\{f_{MR}\} - [H]\{f_c\} + [M][r]\{\ddot{x}_g(t)\} \quad (\text{III.10})$$

$$\frac{[M]}{[M]}\{\ddot{x}(t)\} = -\frac{[C]}{[M]}\{\dot{x}(t)\} - \frac{[K]}{[M]}\{x(t)\} - \frac{[W]}{[M]}\{f_{MR}\} - \frac{[H]}{[M]}\{f_c\} + \frac{[M]}{[M]}\{[r]\}\{\ddot{x}_g(t)\} \quad (\text{III.11})$$

$$\{\ddot{x}(t)\} = -[M]^{-1}[C]\{\dot{x}(t)\} - [M]^{-1}[K]\{x(t)\} - [M]^{-1}[W]\{f_{MR}\} - [M]^{-1}[H]\{f_c\} + [r]\{\ddot{x}_g(t)\} \quad (\text{III.12})$$

The following change of variables is performed:

$$\{x(t)\} = \{x_1(t)\}$$

$$\{\dot{x}(t)\} = \{x_2(t)\} = \{\dot{x}_1(t)\}$$

$$\{\ddot{x}(t)\} = \{\ddot{x}_2(t)\}$$

$$\{U(t)\} = \{U_1(t)\}$$

The following mathematical manipulation are performed:

$$\{U_1(t)\} = -[M]^{-1}[W]\{f_{MR}\} - [M]^{-1}[H]\{f_c\} + [r]\{\ddot{x}_g(t)\} \quad (\text{III.13})$$

$$\begin{cases} \{\dot{x}_1(t)\} = 0\{x_1(t)\} + \{x_2(t)\} + 0\{U_1(t)\} \\ \{\dot{x}_2(t)\} = -[M]^{-1}[C]\{x_2(t)\} - [M]^{-1}[K]\{x_1(t)\} - \{U_1(t)\} \end{cases} \quad (\text{III.14})$$

$$\begin{Bmatrix} \{\dot{x}_1(t)\} \\ \{\dot{x}_2(t)\} \end{Bmatrix} = \begin{bmatrix} 0 & 1 \\ -[M]^{-1}[K] & -[M]^{-1}[C] \end{bmatrix} \begin{Bmatrix} \{x_1(t)\} \\ \{x_2(t)\} \end{Bmatrix} + \begin{Bmatrix} 0 \\ [M]^{-1} \end{Bmatrix} \{U_1(t)\} \quad (\text{III.15})$$

The inputs and output are rearranged in the following form.

$$\dot{z}(t) = \begin{Bmatrix} \{\dot{x}_1(t)\} \\ \{\dot{x}_2(t)\} \end{Bmatrix}, \quad A = \begin{bmatrix} [0] & [I] \\ -[M]^{-1}[K] & -[M]^{-1}[C] \end{bmatrix}, \quad z(t) = \begin{Bmatrix} \{x_1(t)\} \\ \{x_2(t)\} \end{Bmatrix},$$

$$B = \begin{bmatrix} [0] & [I] & [I] \\ [r] & -[M]^{-1}[H] & -[M]^{-1}[w] \end{bmatrix}, \quad U(t) = \{U_1(t)\}, \quad C_c = [I]_{2n \times 2n},$$

$$D = [0]_{2n \times n+1}$$

It is worth noticing that:

- n: number of degrees of freedom (DOF)
- r: number of inputs
- p: number of outputs

III.5. Numerical resolution using MATLAB

this research investigates how a control strategy based on the use of magnetorheological (MR) dampers at different locations in a nonlinear building to enhance its resistance to seismic vibrations. The equation representing the building's motion under seismic excitations is implemented in SIMULINK, a simulation environment, using the State-SpaceToolbox of MATLAB. This toolbox allows working with continuous systems and solving the motion equation. Numerical integration is performed using a high-level solver, the Dormand-Prince solver denoted (OD8), which is integrated with SIMULINK to provide accurate and efficient solutions. An overview of the SIMULINK model for SDOF system is shown in Figure III.11.

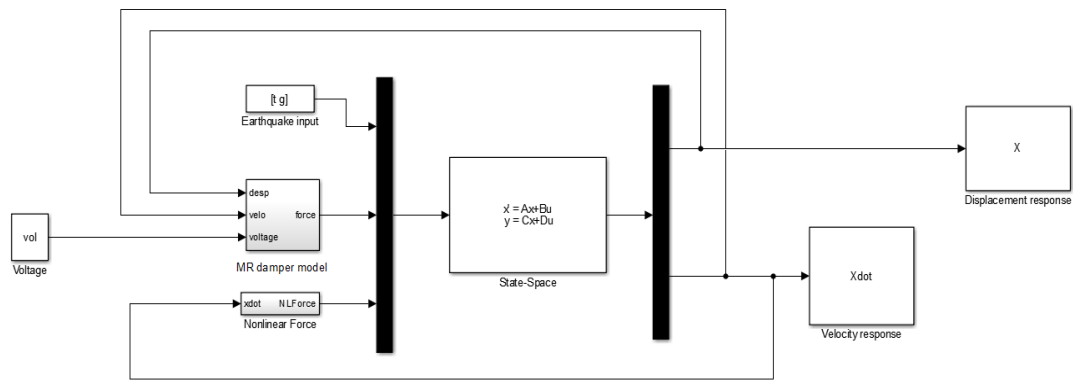


Figure III.11: Simulink file of the used model for a SDOF case

Control strategies are applied so you can compare results obtained under different strategies. This is a control in which a block will be set for the nonlinear response and a block for the damper force under a constant voltage. A manual switch is added to the control scheme in order to switch from controlled to uncontrolled cases. The mathematical equations representing the hysteretic behavior of the structure and the behavior of the MR damper used in this study were reproduced in the SIMULINK scheme using the different blocks of the library proposed by SIMULINK as it can be seen in Figures III.12-III.14.

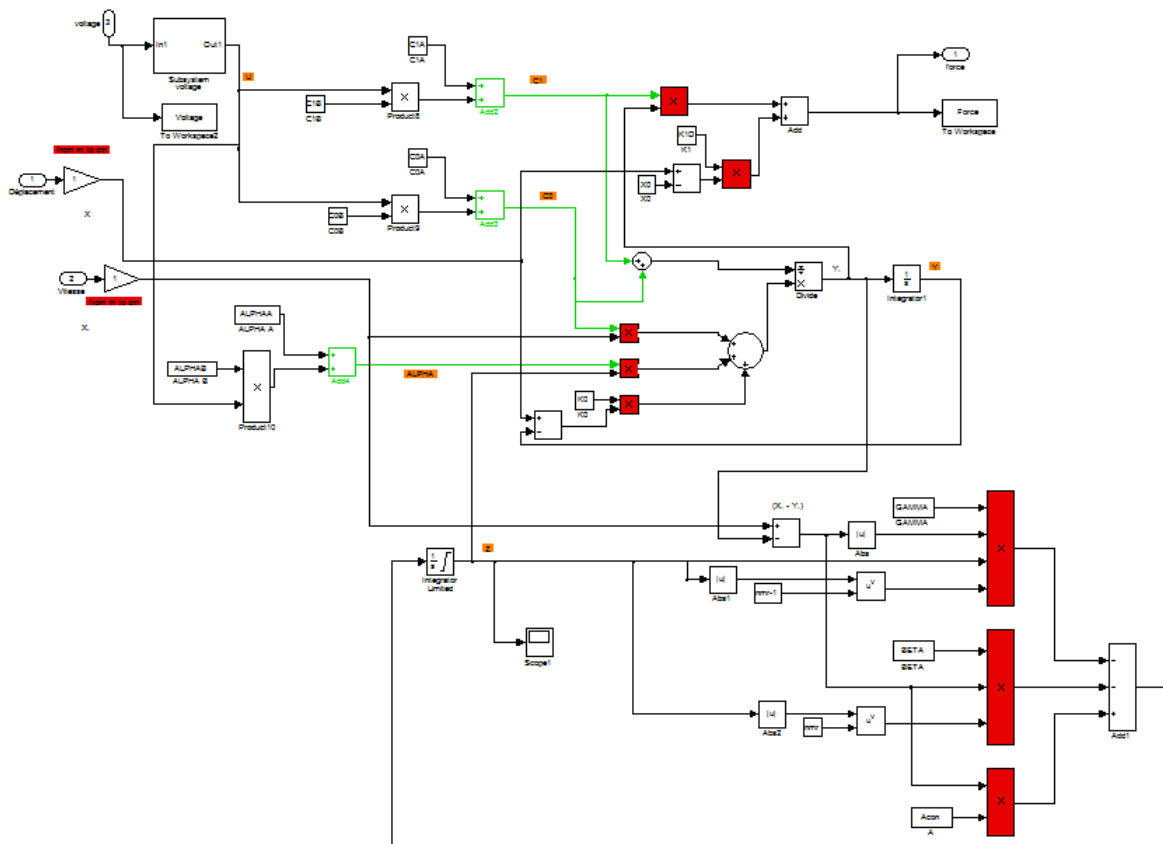


Figure III.12: The MR damper diagram modeled in SIMULINK.[48]

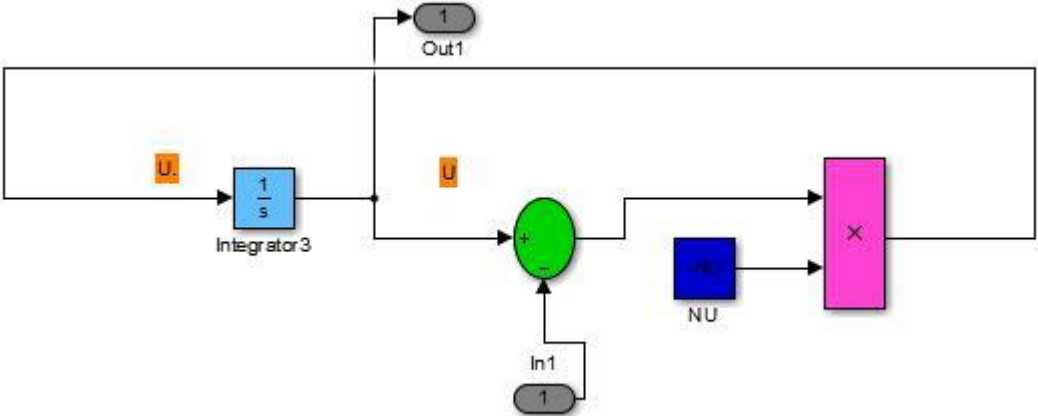


Figure III.13: Modified Simulink MR Bouc-Wen shock absorber file [49]

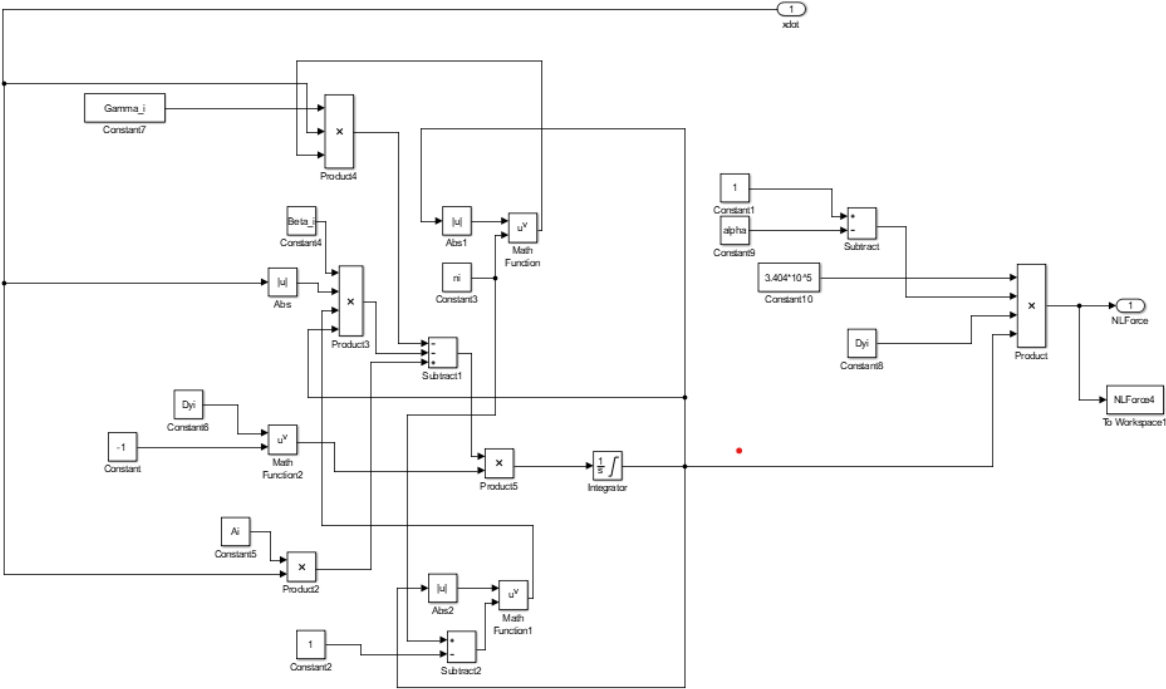


Figure III.14: The nonlinear diagram modeled in SIMULINK

A flowchart of the functioning of the MATLAB code and SIMULINK model is shown in Figure III.15, this later represents the required inputs and the gathered outputs used in the current study.

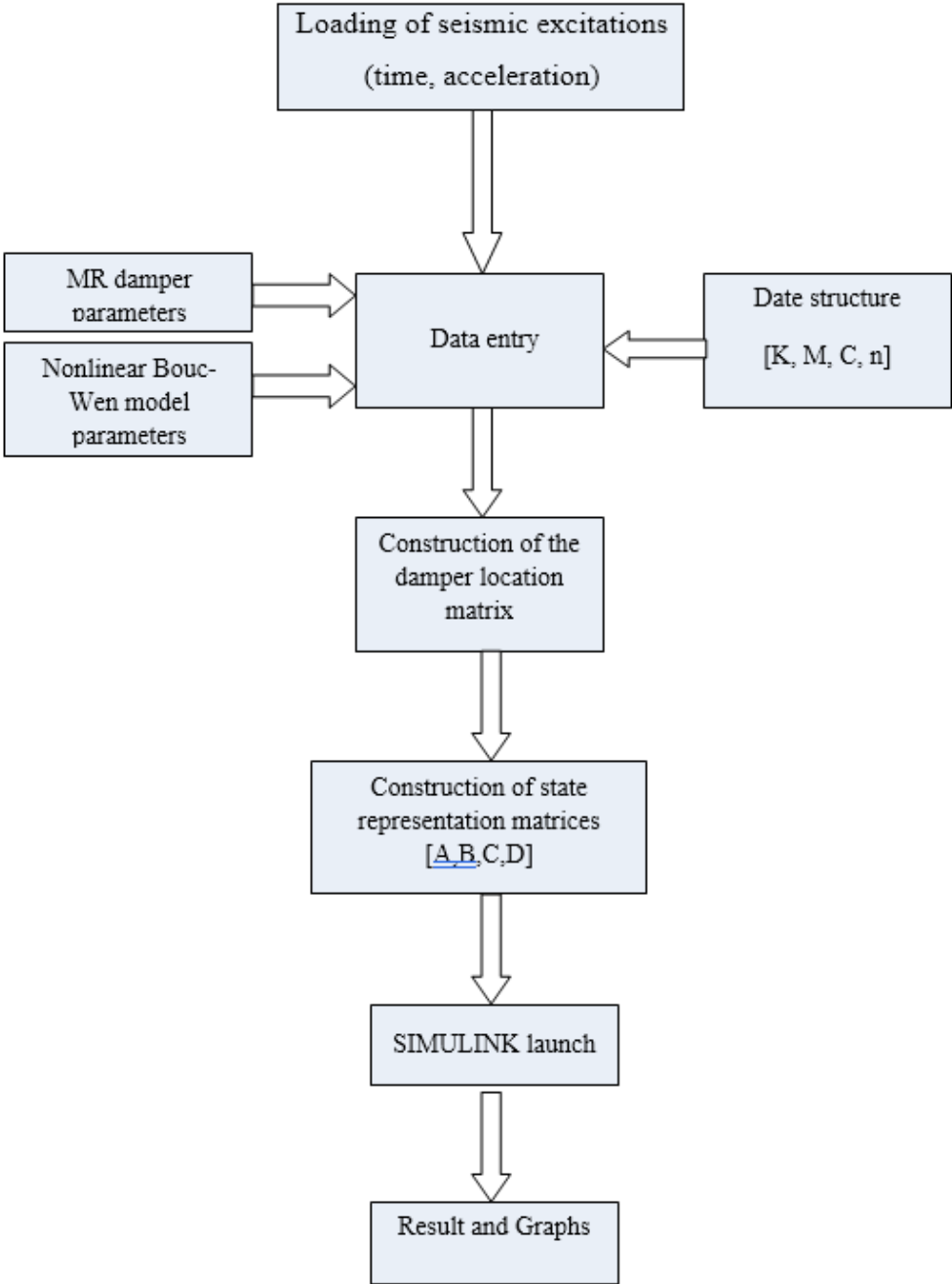


Figure III.15 Flowchart of the simulation used in the current study.

III.6 Conclusion

In this chapter, we have introduced mathematical modeling for controlled and uncontrolled, linear and nonlinear structures where the equations of motion were employed to describe the dynamic behavior of each system. Furthermore, the utilization of state representation, also known as state space, was discussed. In the subsequent chapter, we will apply the state space approach to solve the equations of motion for the considered systems and obtain the dynamical response related to our parameters of interest.

Chapter IV:

Numerical study

Chapter IV: Numerical study

IV.1. Introduction

Building response refers to how a nonlinear or hysteretic structures behaves under external forces such as earthquakes. This chapter presents a numerical study of an eight-story building equipped with MR dampers. The main objective of this study is to investigate the efficiency of a semi-active control strategy on a nonlinear building subjected to a multitude of earthquake records. In this study three different damper configurations will be investigated under three different voltage values. The dynamical parameters of interest examined in this work are: (i) the top floor displacement both in time history and peak values, (ii) the maximum base shear, (iii) the peak drift of all floors, (iv) the peak inter-story drift of all floor, (v) the maximum MR damper force, (vi) the maximum restoring force and (vii) the hysteresis loops.

IV.2. Structural and damper parameters

An eight-story building equipped with MR damper, as shown in (Figure IV.1). The characteristics of the structure are presented in (Table IV.1) and (Table IV.2), the properties of MR damper are presented in (Table IV.3).

The adopted structure for this study was first used by Yang, L [50] as a benchmark model. The building exhibits a nonlinear behavior, to this end, the Bouc-Wen model through equations presented in Chapter II is used to simulate the nonlinear behavior at each of the building floors. Since the mass, stiffness and damping are regularly distributed along the building height each of the Bouc-Wen elements located in all the floors will have the same parameters presented in Table IV.2.

IV.3. Different investigated control strategies

To assess the effectiveness of the MR damper in controlling the seismic response of nonlinear structures, three different damper distribution along the height of the building are adopted. These latter are denoted as follow:

- All floors: where a damper is located in each of the building floors.
- Odd floors: where a damper is placed in odd floors (1st, 3rd, 5th and 7th).
- Even floors: where a damper is placed in even floors (2nd, 4th, 6th and 8th).

In each of the damper location cases three voltage values are applied on all the dampers, these voltage values are 0 Volt, 6 Volts and 12 Volts. Figure IV.1 gives further details on the adopted control strategies.

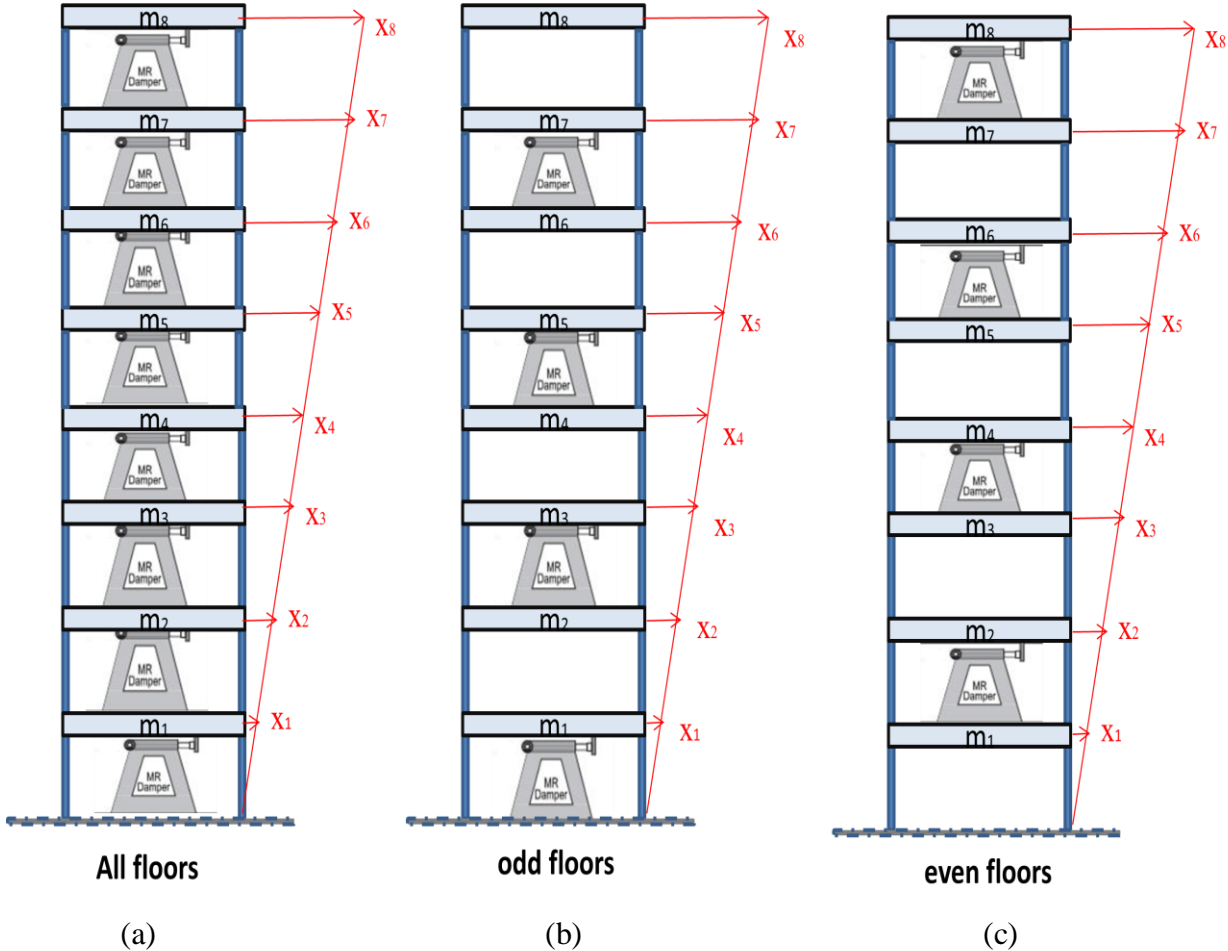


Figure IV.1: Various control strategies(a) all floors, (b) odd floors, (c) even floors

Table IV.1: The properties of the primary structure[51]

Story i	Mass $m_i(t)$ (t)	Stiffness K_i (KN/m.10 ⁵)	Viscous damping Coefficients c_i (KN.s/m)
1	345.6	3.404	734.3
2	345.6	3.404	734.3
3	345.6	3.404	734.3
4	345.6	3.404	734.3
5	345.6	3.404	734.3
6	345.6	3.404	734.3
7	345.6	3.404	734.3
8	345.6	3.404	734.3

Table IV.2: Nonlinear model parameters[52]

Properties	Value
α_i	0.9
D_{yi}	$2.4 \cdot 10^{-2}$ [m]
A_i	1
β_i	0.5
n_i	95
γ_i	0.5

α_i represents the post-to-pre yield stiffness ratio, D_{yi} is the yield displacement, A_i, β_i and γ_i are dimensionless parameters that govern the shape of the restoring force and the scale of the hysteresis loop

Table IV.3: The properties of MR damper

Properties	Value	Unit
C_{0A}	2012	$kN.s.m^{-1}$
C_{0B}	487.0	$kN.s.m^{-1}$
K_0	0.0054	$kN.s.m^{-1}$
C_{1A}	81062	$kN.s.m^{-1}$
C_{1B}	78089	$kN.s.m^{-1}V$
K_{1D}	0.0087	$kN.m^{-1}$
α_A	8.70	$kN.m^{-1}$
α_B	6.40	$kN.m^{-1} V$
Γ_{MR}	496	m^{-2}
β_{MR}	496	m^{-2}
η	195	s^{-1}
x_0	0	m

IV.4. Description of seismic excitations

The building studied in this work will be subjected to the following seismic excitations:

- El Centro earthquake of 1940, with a magnitude of 6.9 and a maximum ground acceleration with a PGA of 0.34g.
- Lexington earthquake of 1989, with a magnitude of 6.9 and a maximum ground acceleration with a PGA of 0.42g.
- Kobe earthquake of 1995, with a magnitude of 6.9 and a maximum ground acceleration with a PGA of 0.62g.
- Northridge earthquake of 1994, with a magnitude of 6.7 and a maximum ground acceleration with a PGA of 0.82g.

The choice of these four recordings is motivated by their characteristics; El Centro and Lexington are considered in the literature as far-field earthquakes, while Northridge is considered as a near-field earthquake with a directivity effect, and Kobe is considered as a near-field earthquake with a significant ground displacement effect (pulse-like records).

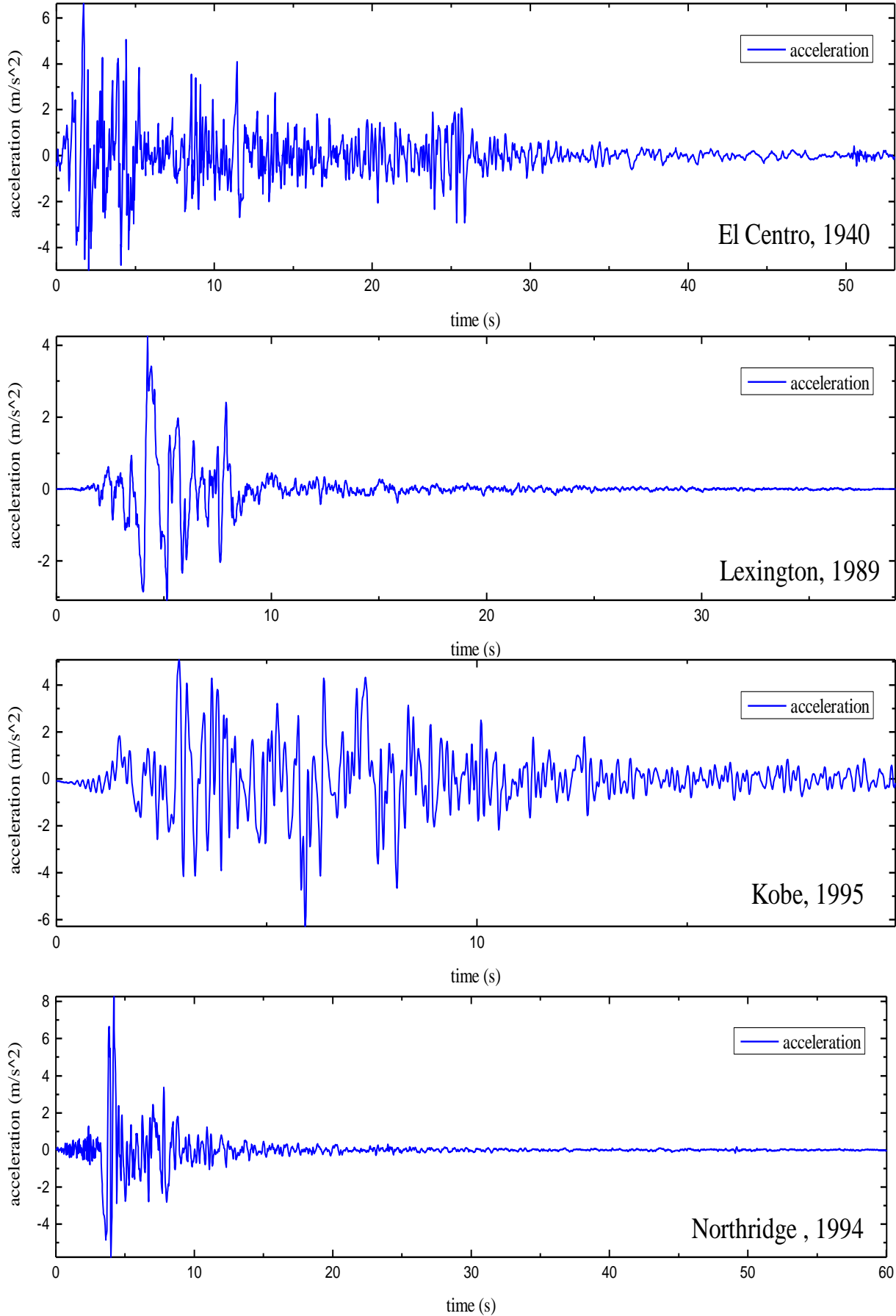


Figure IV.2:Earthquakes record used in this study

IV.5. Results and discussion

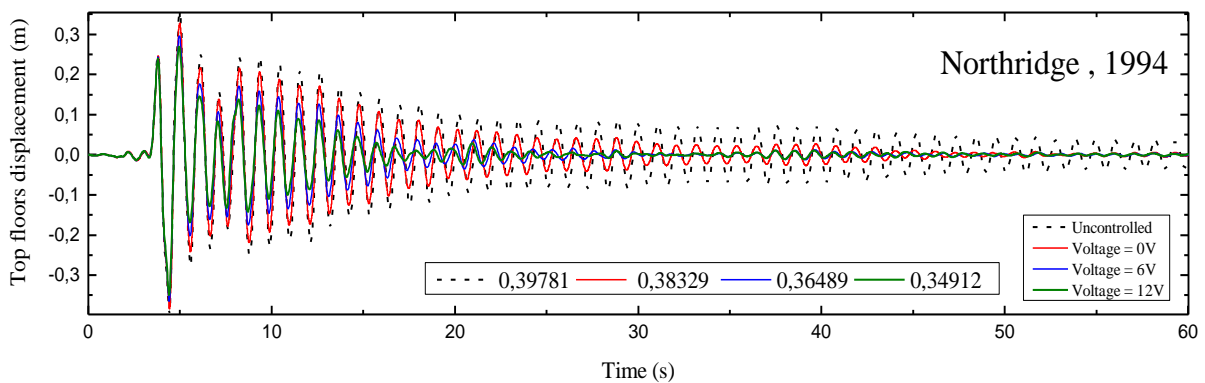
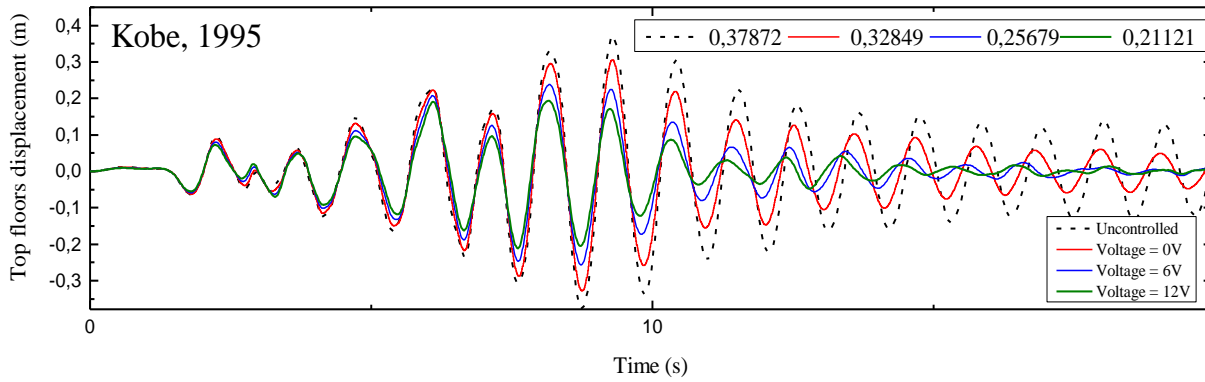
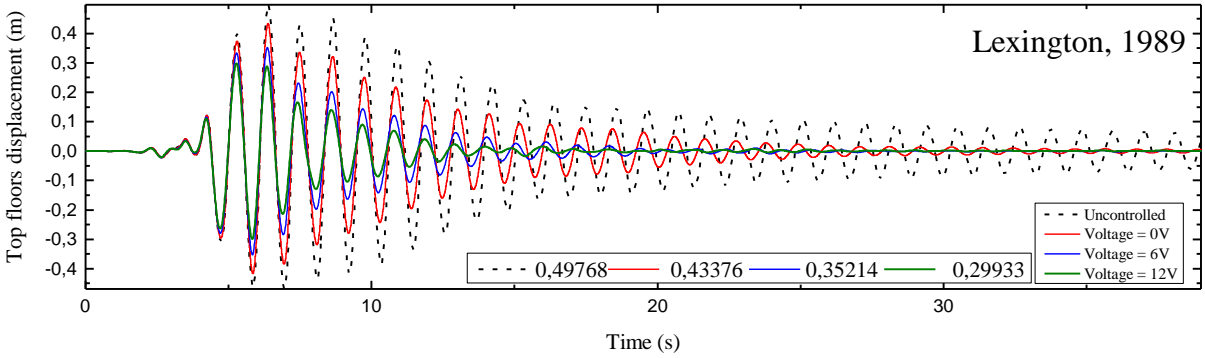
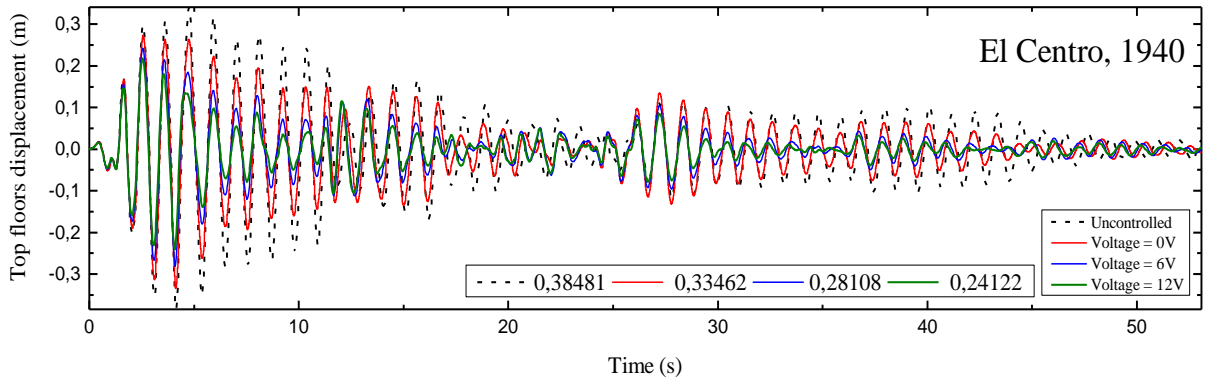
IV.5.1. Peak top floor displacement and time history under various control strategies

Table IV.4 presents the results obtained for the peak top floor displacement under various control strategies, under different seismic excitations combined with multiple voltage values applied to the damper (MR).

Table IV.4: Peak displacement under various control strategies [m]

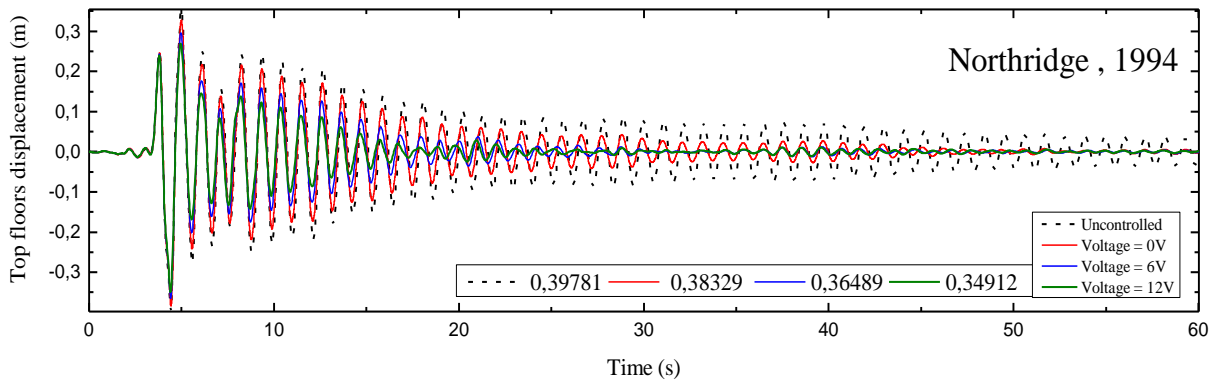
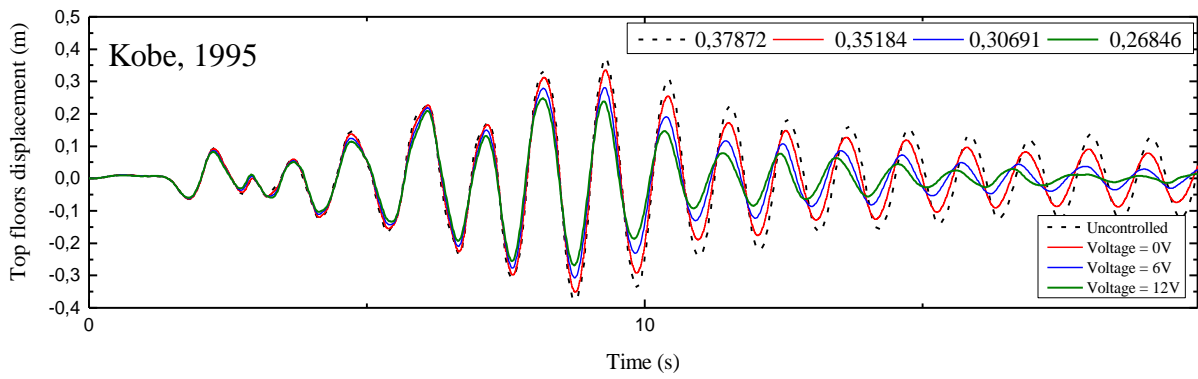
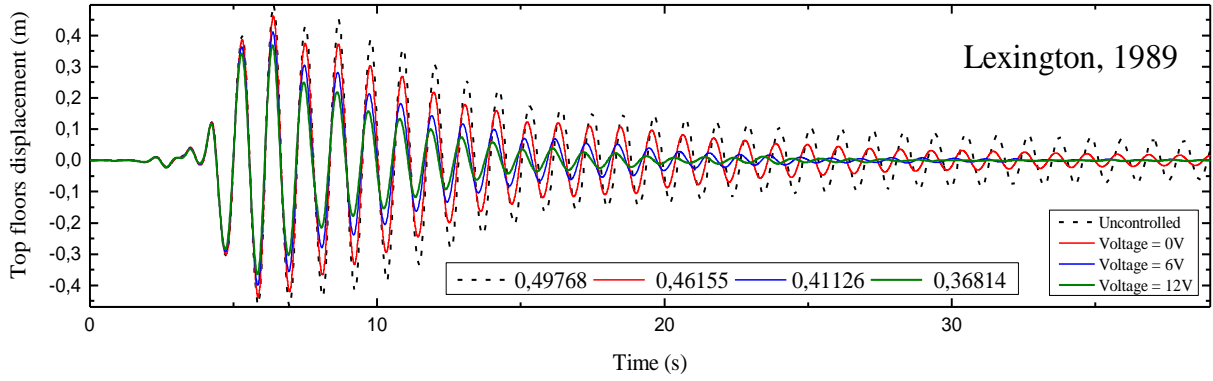
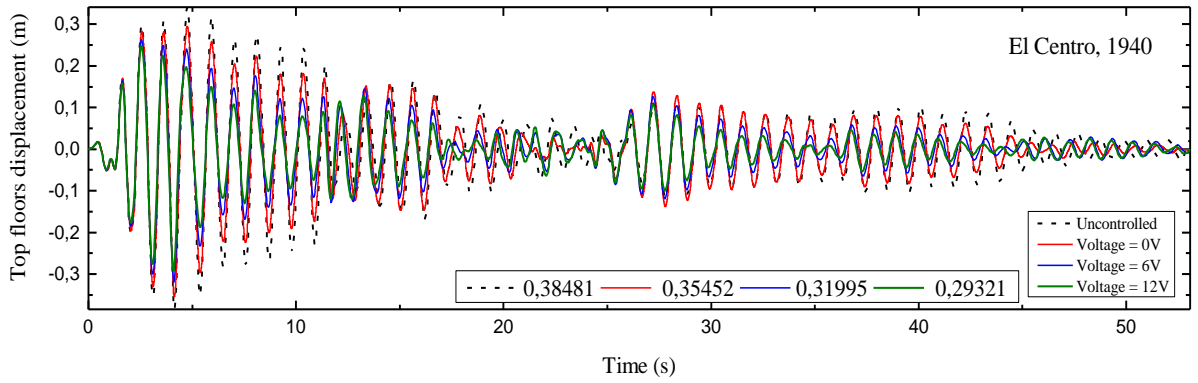
Earthquake	Voltage	Without control device	With control device		
			All floors	Odd floors	Even floors
El Centro, 1940	V=0	0,3848	0,3346 13,04 %	0,3545 7,86%	0,3599 6,45%
	V=6		0,2810 26,95%	0,3199 16,85%	0,3320 13,71%
	V=12		0,2412 37,31%	0,2932 23,80%	0,3088 19,72%
Lexington, 1989	V=0	0,4976	0,4337 12,84%	0,4615 7,25%	0,4692 5,71%
	V=6		0,3521 29,24%	0,4112 17,36%	0,4288 13,82%
	V=12		0,2993 39,85%	0,3681 26,02%	0,3931 20,99%
Kobe, 1995	V=0	0,3787	0,3284 13,26%	0,3518 7,09%	0,3575 5,57%
	V=6		0,2567 32,19%	0,3069 18,96%	0,3220 14,96%
	V=12		0,2112 44,23%	0,2684 29,11%	0,2898 23,45%
Northridge, 1994	V=0	0,3978	0,3722 6,43%	0,3832 3,64%	0,3864 2,84%
	V=6		0,3413 14,19%	0,3648 8,27%	0,3713 6,64%
	V=12		0,3141 21,03%	0,3491 12,23%	0,3589 9,77%

In Table IV.1, it is evident that the first control strategy namely all floors' results in superior response reduction with respect to the response of the structure without a damper; this observation is valid across all four seismic excitations used. Regarding the voltage applied to the damper, the maximum value (12V) ensures the highest reduction. The best percentage reduction of the top floor displacement is recorded under Kobe, 1995 records with 44.23%. From the Table IV.1, it is also clear that the second-best control strategy is the odd floors followed by the even floor damper distribution.

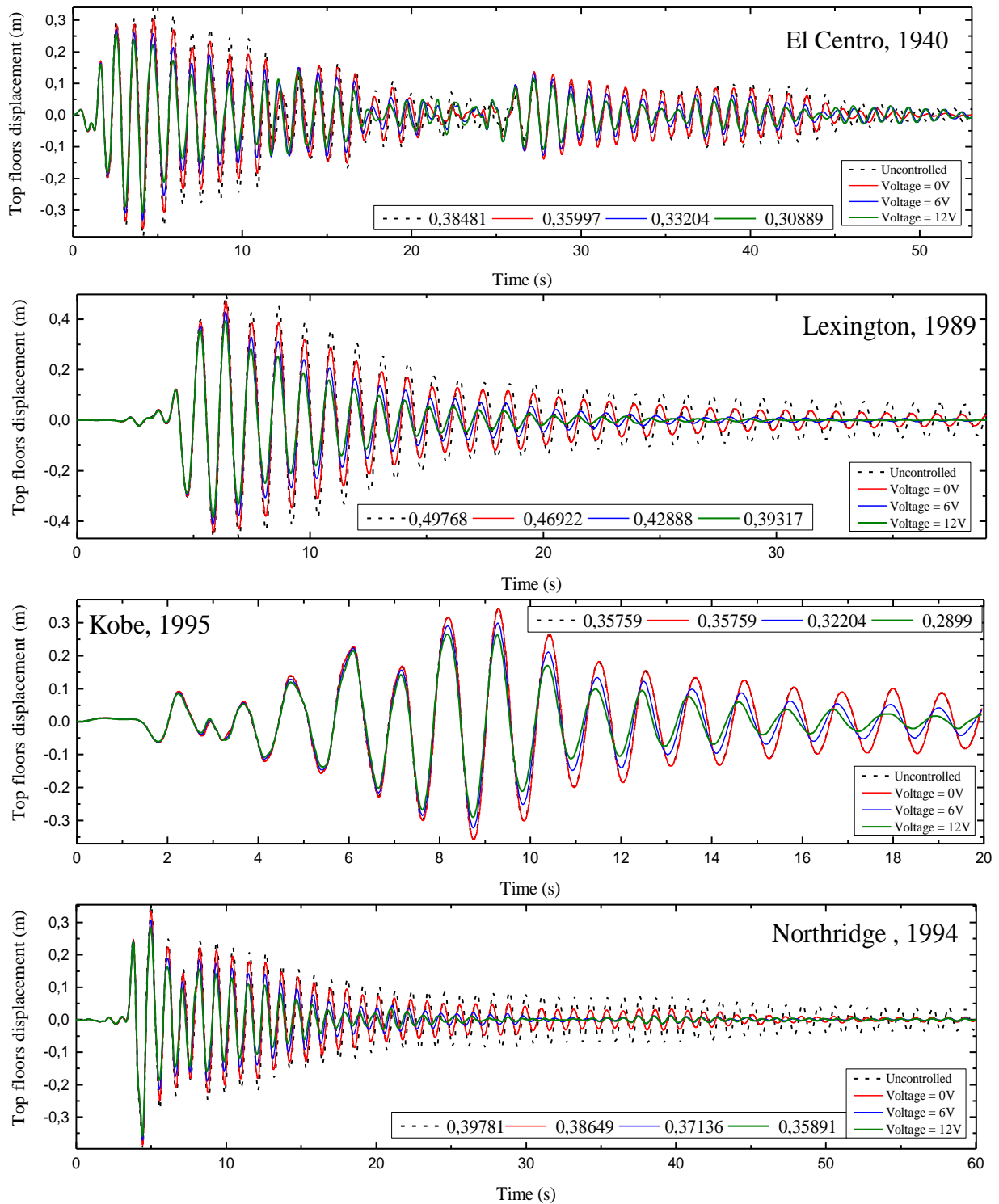


(a) All floors

Chapter IV: Numerical study



(b) Odd floors



(c) Even floors

Figure IV.3: Time history of Top floor displacement under various control strategies

Figures IV.3 which shows the time history of top floor displacement under different used seismic excitations. It confirms the results outlined in Table IV.4, demonstrating that the first control strategy outperforms the other control strategies. Notably, when the voltage is zero, the effectiveness of the damper is barely noticeable across all seismic excitations. Further it

can be seen that the top floor displacement is reduction along the time totality of the time history. Using high voltage will dampen the structure motion quickly, which will prevent cyclic loading and damages to the structural elements.

IV.5.2. Base shear at the base

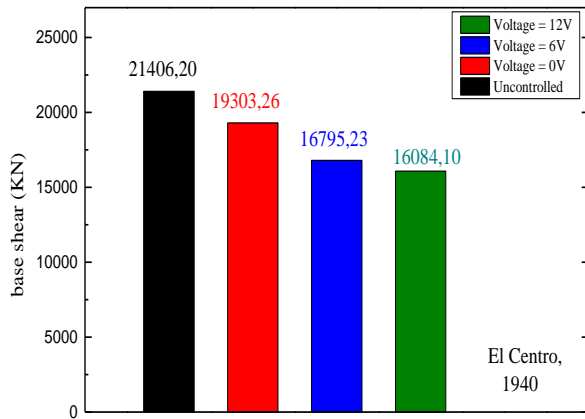
Table IV.5 presents the maximum base shear of the examined building for the utilized damper locations, across different seismic excitations coupled with varying voltage levels applied to the magnetorheological (MR) damper.

Table IV.5: Maximum base shear[kN]

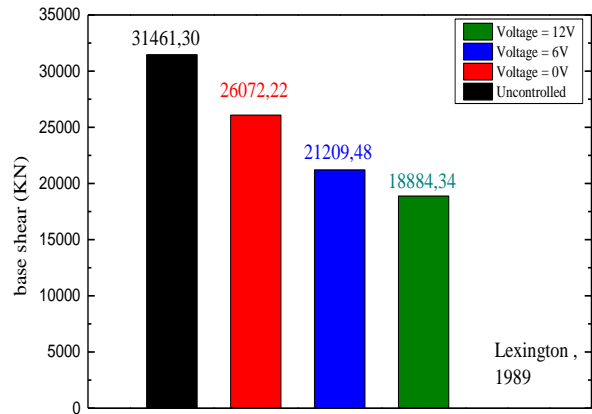
Earthquake	Voltage	Without control device	With control device		
			All floors	Odd floors	Even floors
El Centro, 1940	V=0	21406.20	19303.25 9.82%	20304.19 5.14%	20513.57 4.16%
	V=6		16795.23 21.54%	18628.77 12.97%	19209.35 10.26%
	V=12		16084.09 24.86%	17530.82 18.10%	18098.59 15.45%
Lexington, 1989	V=0	31461.29	26072.21 17.12%	28087.70 10.72%	28756.82 8.59%
	V=6		21209.48 32.58%	24518.81 22.06%	25768.04 18.09%
	V=12		18884.34 39.97%	22099.40 29.75%	23679.16 24.73%
Kobe, 1995	V=0	26795.48	20837.23 22.23%	22882.06 14.60%	23644.66 11.75%
	V=6		16392.35 38.82%	19310.51 27.93%	20480.81 23.56%
	V=12		14178.66 47.08%	16809.28 37.26%	18489.50 30.99%
Northridge, 1994	V=0	28937.92	26575.50 8.16%	27562.52 4.75%	27923.14 3.50%
	V=6		23944.79 17.25%	25921.54 10.42%	26586.65 8.12%
	V=12		21921.46 24.24%	24533.62 15.21%	25518.16 11.81%

Table IV.5 presents the maximum shear force at the base of the studied structure under various seismic excitations. Across the three studied strategies, it's evident that the first strategy yields superior results compared to the uncontrolled structure's response (without dampers). Regarding the voltage applied to the damper, the maximum value (12V) ensures the greatest reduction. The maximum reduction percentage is (47.08%), achieved for the Kobe, 1995 earthquake while using the all-floors strategy with a maximum voltage (12V).

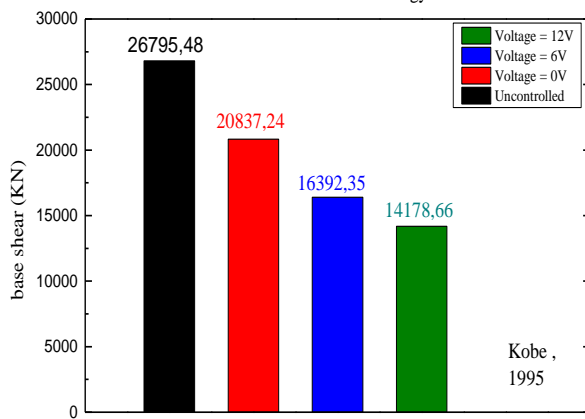
Chapter IV: Numerical study



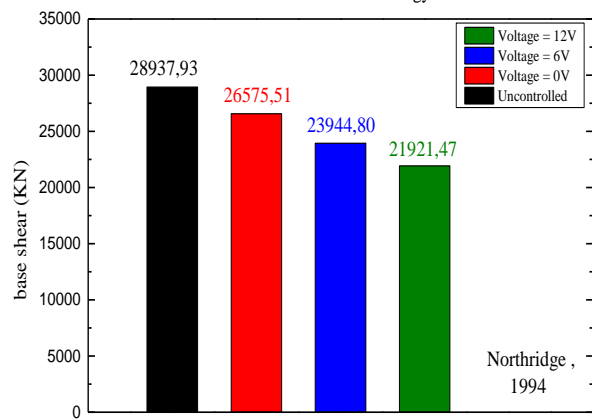
Different control strategy



Different control strategy

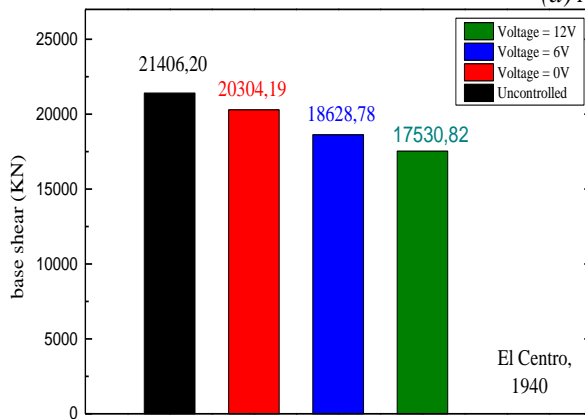


Different control strategy

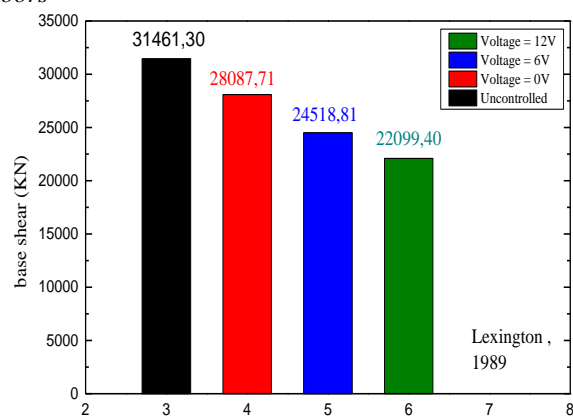


Different control strategy

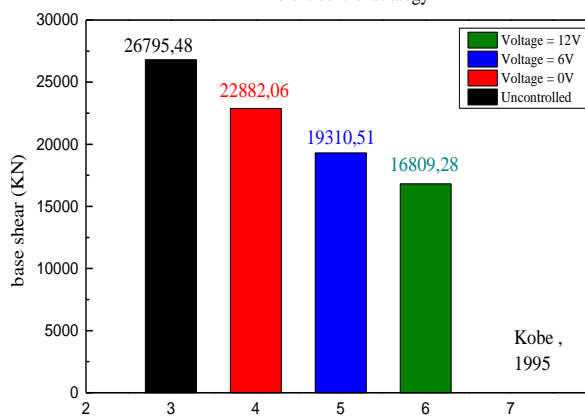
(a) All floors



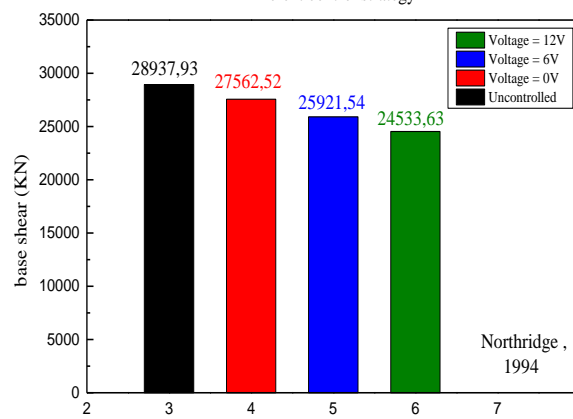
Different control strategy



Different control strategy

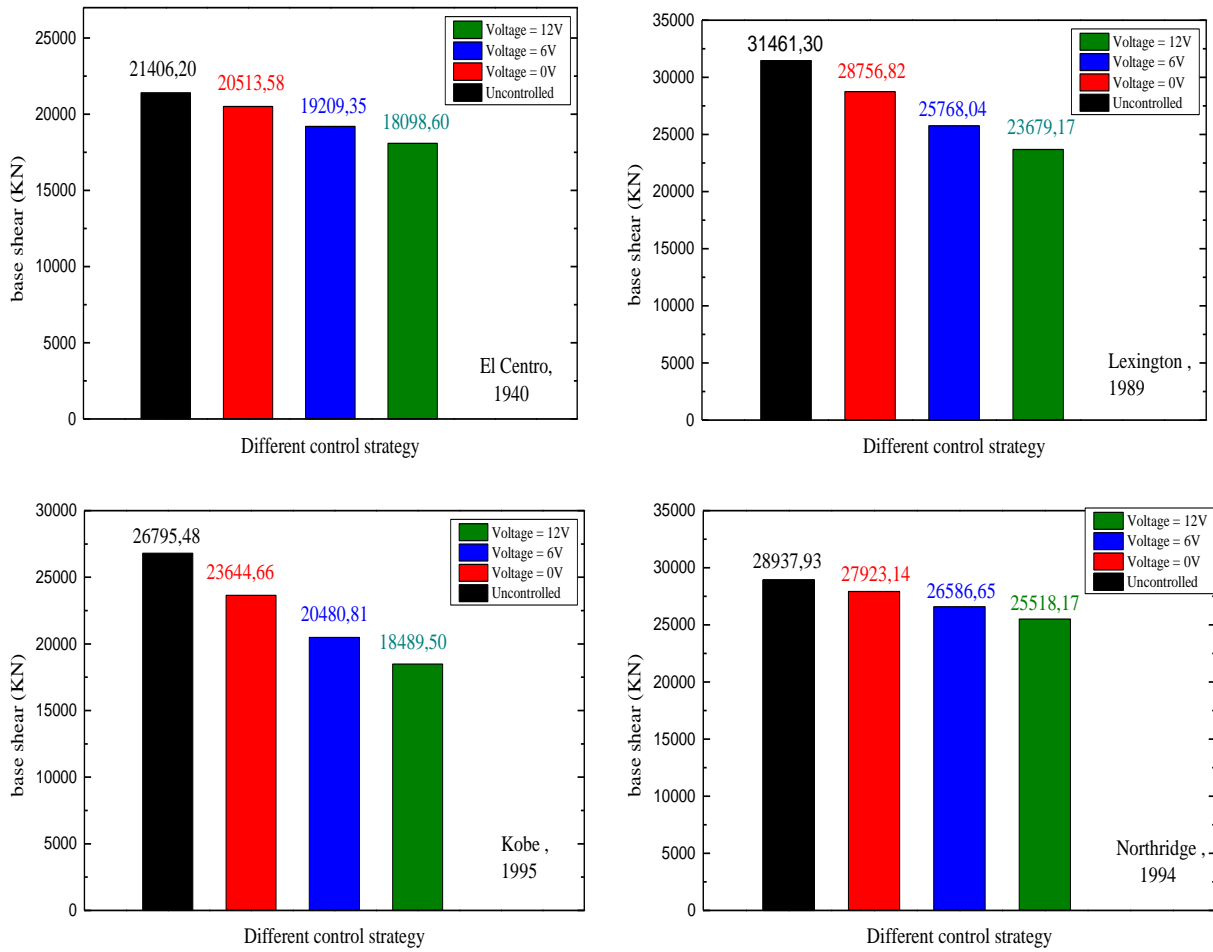


Different control strategy



Different control strategy

(b) Odd floors

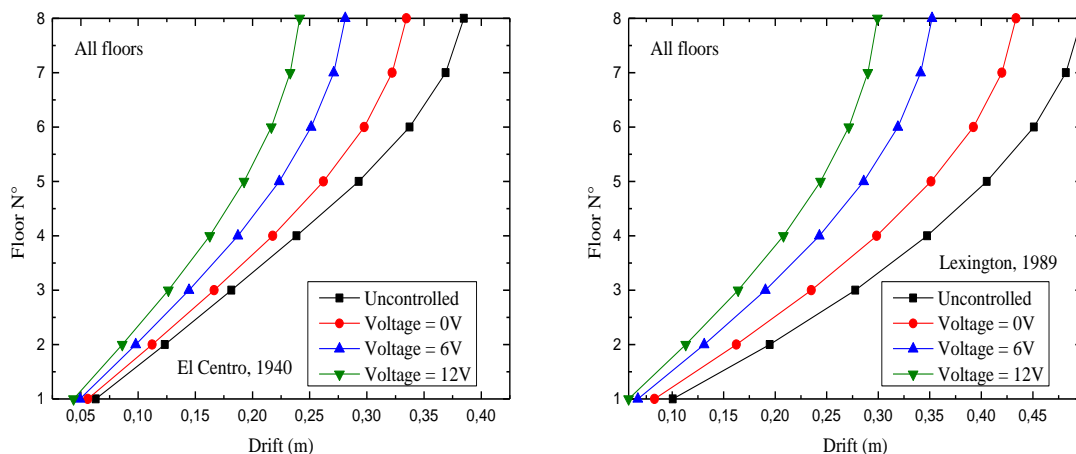


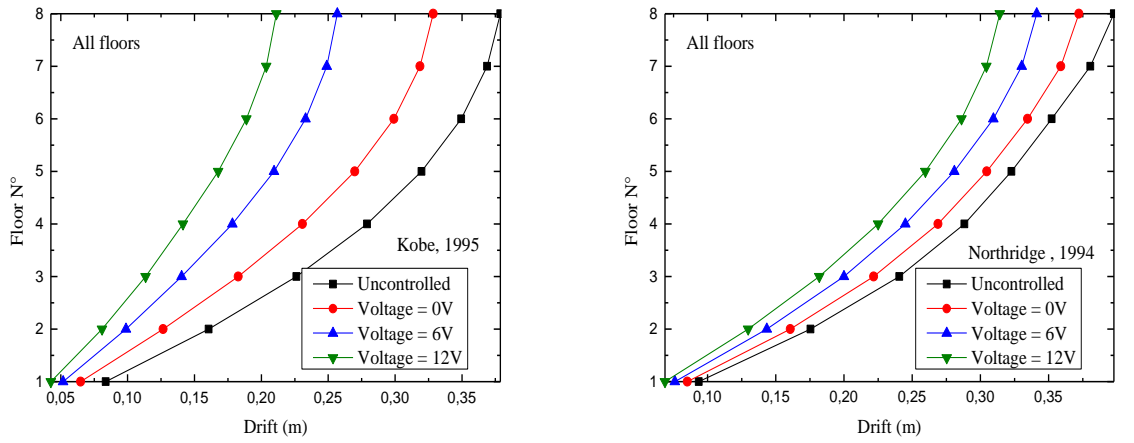
(c) Even floors

Figure IV.4: Base shear at the base under different control strategies

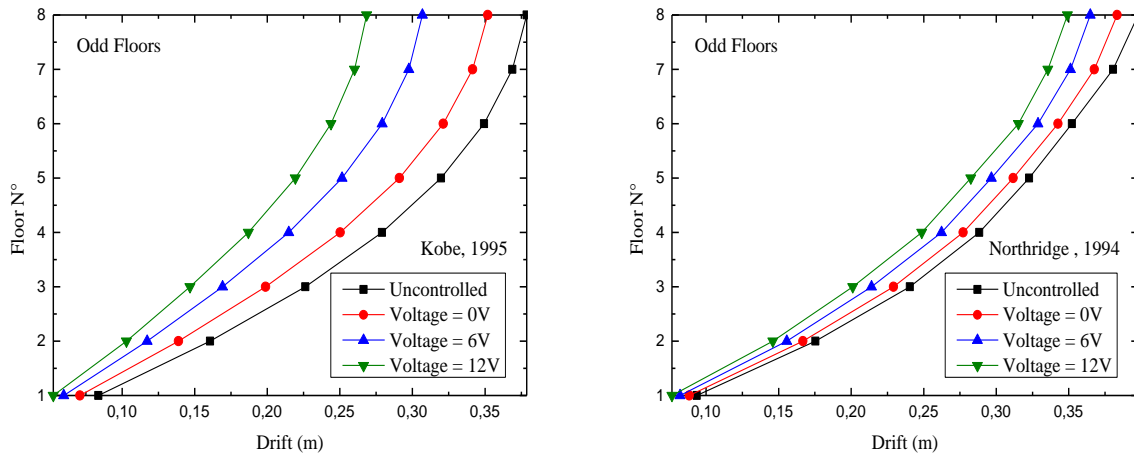
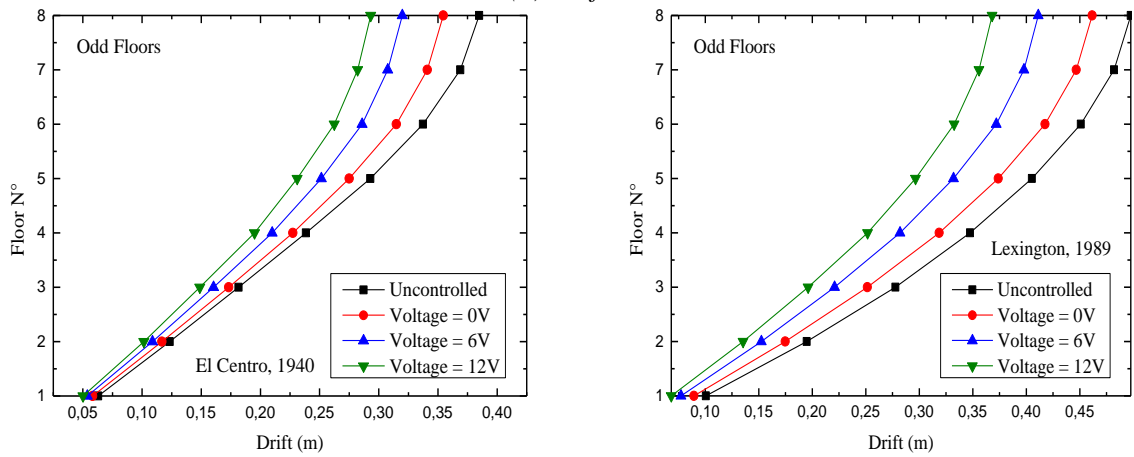
Figures IV.4 illustrate the reduction in shear force at the base of the studied building under the four selected seismic excitations. The first strategy of MR damper placement demonstrates superior reductions compared to the other placement variants, with the optimal voltage value being 12V. This confirms the results shown in Table IV.5.

IV.5.3. Peak drift values of all the floors under different control strategies

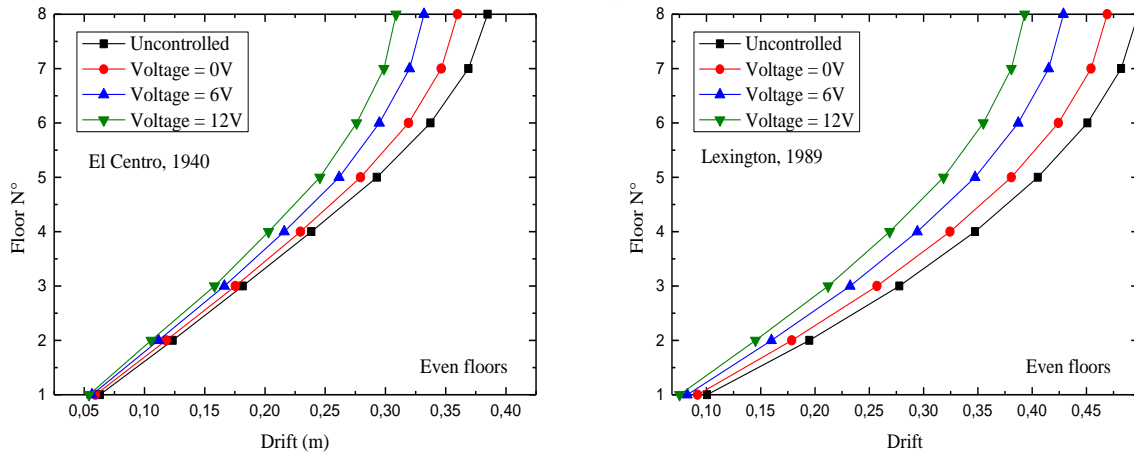


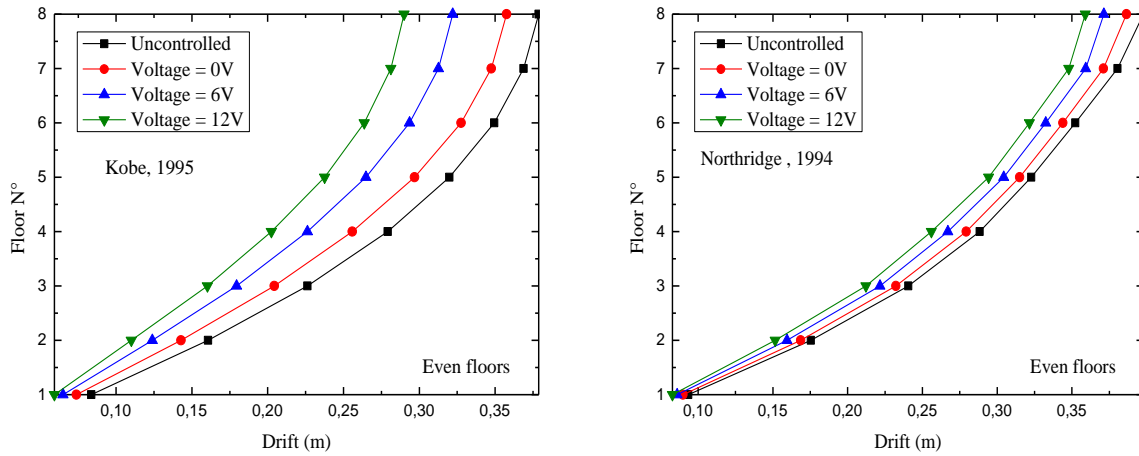


(a) All floors



(b) Odd floors





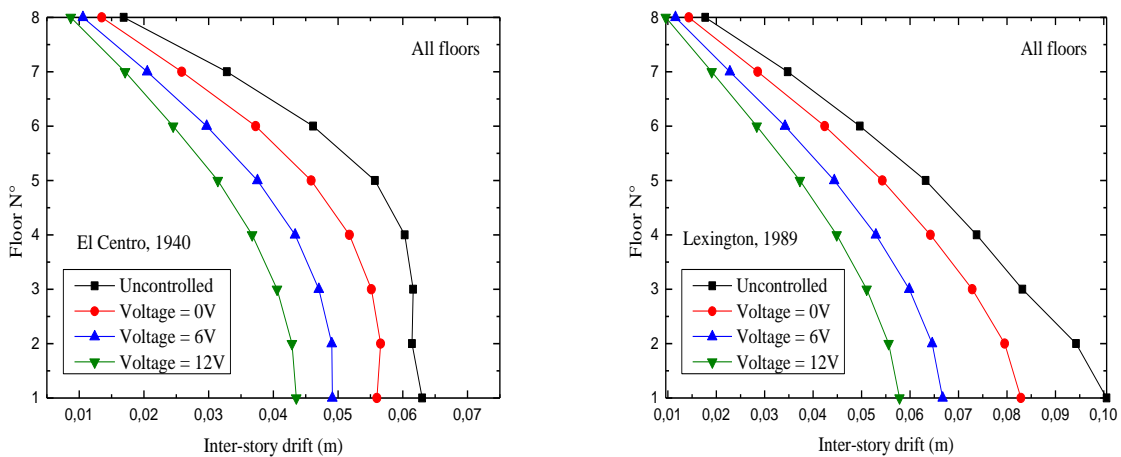
(c) Even floors

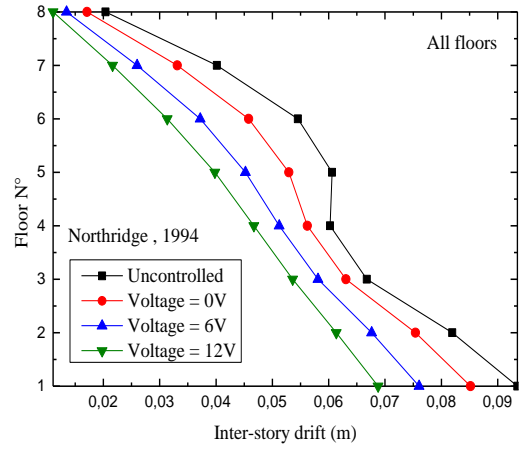
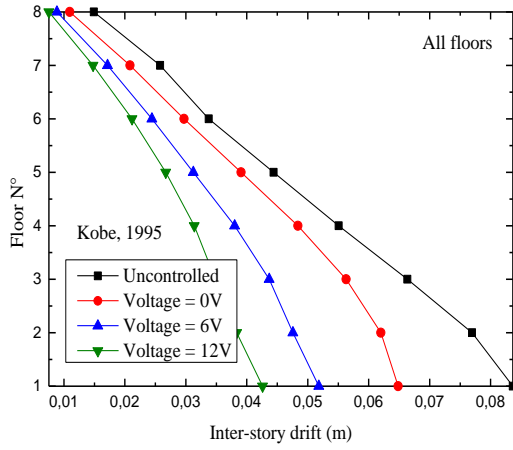
Figure IV.5. Peak drift values of all the floors under different control strategies

Figure IV.5 shows the peak story drift of all the floors under the selected seismic records while applying various control strategies with various voltage values. It is clearly that the introduction of MR damper reduces the maximum drift of all the floors. It is clear that the high voltage results in better reduction while damper placement in all the floors ensures the best response reduction. On the other hand, alternation of the damper location does not disrupt the drift response.

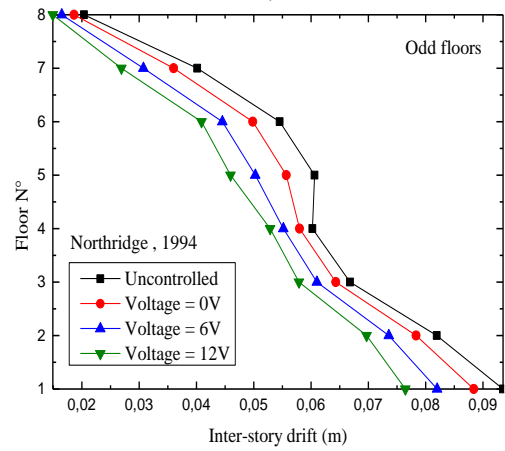
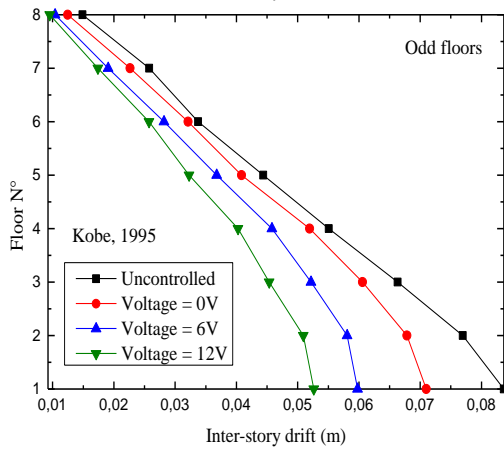
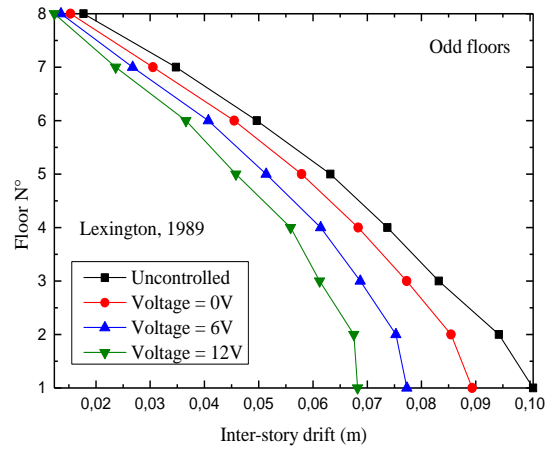
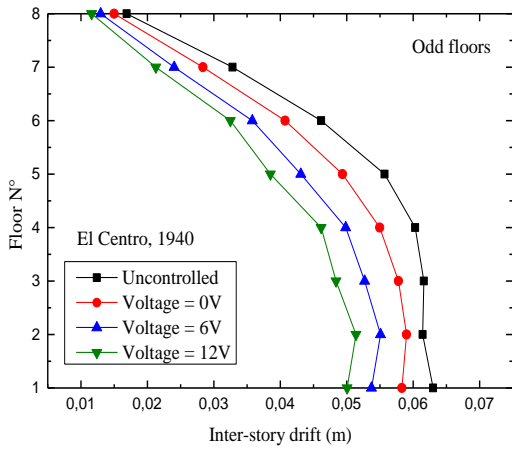
IV.5.4. Peak inter-story drift under different control strategies

The plots shown in Figure IV.6 illustrate the maximum inter-story displacements of the studied building under the investigated control strategies, across various seismic excitations combined with multiple voltage values applied to the magnetorheological (MR) damper. It is important to mention that the inter-story drift is a very important parameters that help assessing the efficiency of a damper seismic response control. Further an inter-story drift less than the yield displacement will keep the floor in the elastic domain.

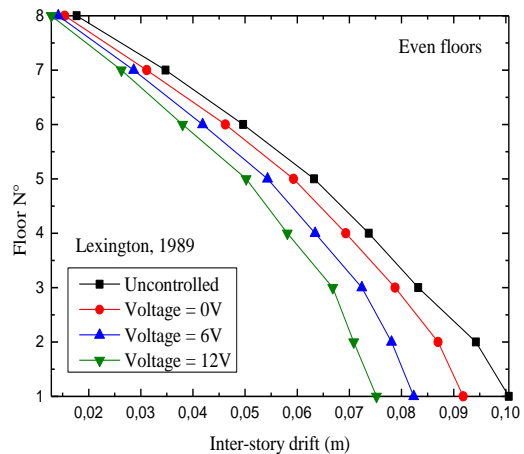
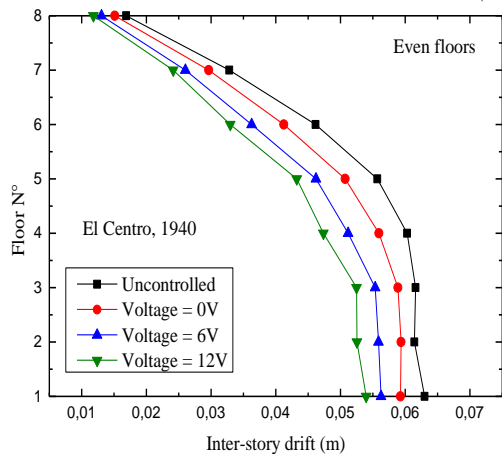


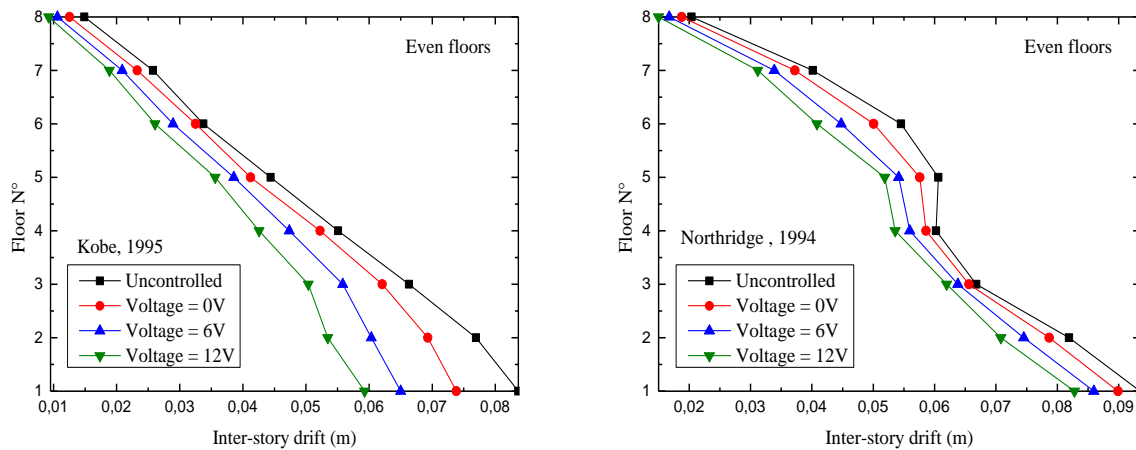


(a) All floors



(b) Odd floors





(c) Even floors

Figure IV.6: Peak inter-story drift under different control strategies

Figure IV.6. shows the inter-story drift of all the floors for the uncontrolled structure and the structure controlled with MR damper with various damper distribution and applied voltages. It can be seen that there always a reduction in the inter-story drift especially when using high voltage values. The quantity of the reduction varies from an earthquake to another. It is worth noticing that reducing the inter-story drift prevents the floor from undergoing nonlinear behavior hence considerably reducing the risk of shear failure.

IV.5.5. Peak MR damper force

Table IV.6 shows the maximum force produced by the MR damper.

Table IV.6: Peak MR damper force [kN]

Earthquake	Voltage	All floors	Odd floors	Even floors
El Centro, 1940	V=0	788,07	867,85	887,66
	V=6	1591,07	1809,01	1993,45
	V=12	2223,46	2603,92	2942,22
Lexington, 1989	V=0	928,54	980,38	996,08
	V=6	1967,47	2265,65	2342,66
	V=12	2671,51	3372,25	3618,33
Kobe, 1995	V=0	742,14	778,81	865,47
	V=6	1582,41	1818,25	2106,22
	V=12	2233,95	2632,23	3267,28
Northridge, 1994	V=0	1020,72	1107,47	1155,53
	V=6	2017,92	2432,40	2582,52
	V=12	2760,76	3414,70	3875,84

Table IV.6 illustrates the peak force generated by the dampers across each variant amidst the four seismic excitations. The type of seismic activity significantly influences the peak force generated by the dampers. In instances of distant earthquakes (El Centro), we observe a relatively modest force output ranging between 700 and 3000 [kN]. Conversely, during nearby seismic events like Kobe and Northridge, the dampers exhibit a force output surpassing 3000 [kN]. It is also worth noticing that the control strategies resulting in the highest damper force don't result necessarily in the best response reduction. This shows that high control force does not always result in best reduction.

IV.5.6. Peak restoring force of the first floor under various control strategies

Table IV.7: Maximum restoring force[kN]

Earthquake	Voltage	Without control device	With control device		
			All floors	Odd floors	Even floors
El Centro, 1940	V=0	20118,91	18146,84 9,80%	18895,87 6,07%	19002,57 5,54%
	V=6		15868,68 21,12%	17695,50 12,04%	18055,95 10,25%
	V=12		14155,29 29,64%	16558,91 17,69%	17353,68 13,74%
Lexington, 1989	V=0	31628,44	26208,42 17,13%	28190,90 10,86%	28955,68 8,45%
	V=6		21256,54 32,79%	24497,21 22,54%	26043,48 17,65%
	V=12		18528,44 41,41%	21714,59 31,34%	23853,93 24,58%
Kobe, 1995	V=0	26443,64	20683,22 21,78%	22568,58 14,68%	23439,27 11,36%
	V=6		16688,26 36,89%	19129,55 27,65%	20730,56 21,60%
	V=12		13866,14 47,56%	16938,74 35,94%	18985,36 28,20%
Northridge, 1994	V=0	29458,88	26913,11 8,64%	27896,49 5,30%	28347,61 3,77%
	V=6		24110,42 18,15%	25933,27 11,96%	27152,03 7,83%
	V=12		21880,41 25,72%	24237,08 17,72%	26181,85 11,12%

IV.5.7. HysteresisLoop

A Hysteresis Loop representing the relationship between displacement, velocity and the restoring force with both its components (linear and nonlinear) under seismic excitation on a nonlinear building is a crucial tool for analyzing and understanding the structural behavior under dynamic loads with and without control device. This loop reveals the mechanical and structural properties of the building, helping to evaluate its seismic performance and stability. Hysteresis loops can be drawn with respect to relative velocity or relative displacement, the surface of each loop represents the energy dissipated.

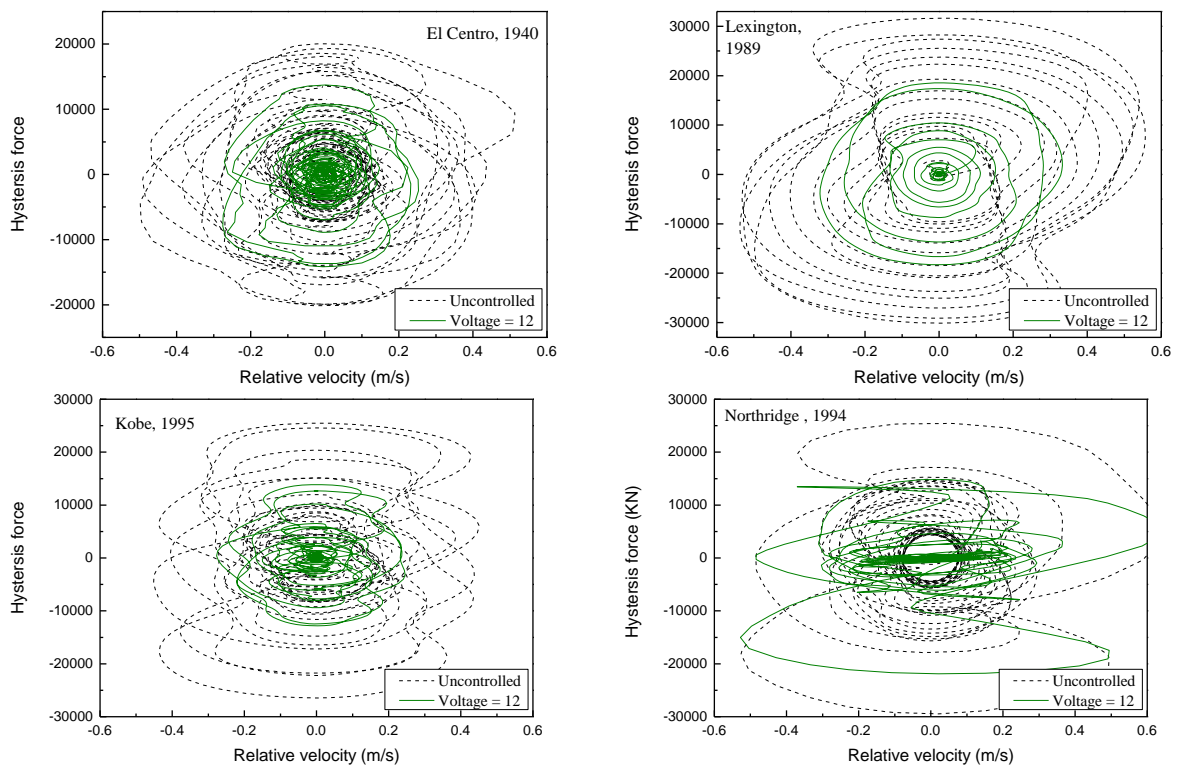


Figure IV.7: hysteresis loop in terms of relative velocity

In Figure IV.7, which represents the velocity versus hysteresis force in the first floor of the studied building under the all-floors control strategy. We observe that the hysteresis force loop decreases when the voltage is 12 Volts in the presence of a damper, compared to the absence of a damper. This decrease is noticeable across all the proposed seismic excitations. Also, it can be seen that the velocity is reduced. Earthquakes with strong pulse motion such as Northridge may result in irregular shape of hysteresis loops.

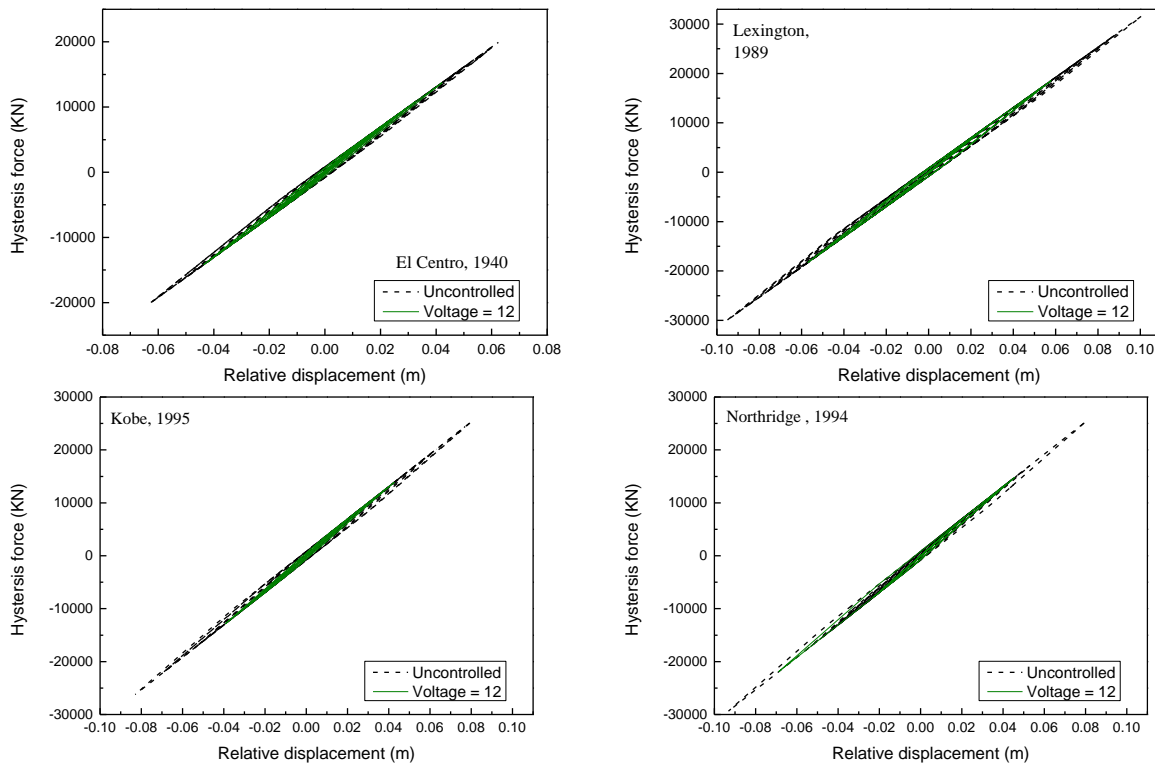


Figure IV.8: hysteresis loop in terms of displacement

From the hysteresis loops with respect to the relative displacement shown in Figure IV.8, we observe that the surface areas of the loops decrease from the case of uncontrolled to the case of having a damper at a voltage of 12 volts. It is worth noticing that these loops are plotted for the hysteresis force at the first floor for the control strategy involving a damper at each of the building's floors. It is worth noticing that for the controlled case the relative displacement and also the hysteresis force notably reduces which proves the importance and efficiency of the control strategy.

IV.6. Conclusion

In conclusion, it can be said that the seismic performance of a nonlinear building equipped with MR dampers was studied. The study involved three different control strategies related to the MR damper distribution along the building height. For each of the control strategies various voltages were applied to the damper; this resulted in an extensive parametric study.

The MR damper proved to be an effective mean for reducing the seismic response of structures exhibiting nonlinear behavior, in terms of peak top floor displacement the response was reduced up to 44% compared to the uncontrolled case.

Further, the peak base shear was up to 47% with respect to the uncontrolled case which is a good indicator of the MR damper efficiency. Since the base shear is strongly related to the

relative acceleration, its reduction is synonym of a good acceleration reduction. Similarly, the drift, inter-story drift and hysteresis forces were considerably reduced preventing the building from exhibiting irreversible damage. All the above-mentioned results prove the performance of the MR damper in reducing the seismic response of nonlinear buildings.

General conclusion

General conclusion

In this thesis, we investigated the effectiveness of semi-active control using a magnetorheological (MR) damper for the seismic response of a nonlinear structure. The MR damper was implemented in an 8-story mid-rise structure exhibiting nonlinear behavior through a restoring force represented using a Bouc-Wen hysteresis model. The structure was equipped with MR dampers following three various placement configurations. The building was subjected to various seismic excitations. The conclusions from this study are summarized as follows:

- **Improved Structural Performance:** The MR damper significantly enhanced the building's overall structural performance during seismic events. It effectively reduced displacements, base shear, drift and inter-story drifts, contributing to the stability and safety of the structure.
- **Damper location and voltage variations:** The study examined the damper's effectiveness at different location through three distribution schemes, also three voltages values were applied on the damper (12V, 6V, and 0V). Placing a damper at each of the building floor combined with a higher voltage generally resulted in better damping performance. It is worth noticing that event at lower voltages, the damper could ensure a certain response reduction.
- **Energy Dissipation:** The MR damper efficiently dissipated seismic energy, thereby minimizing the force transmitted to the structure. This resulted in lower hysteresis forces preventing the structure from undergoing nonlinear behavior.

These conclusions underscore the potential of MR dampers in improving the seismic performance of structures, making them a valuable addition to earthquake-resistant design strategies, especially when considering structures with nonlinear behavior.

As a perspective, a control algorithm could be introduced to vary the voltage simultaneously during the earthquake excitation. Further, an optimization algorithm can be applied to decide the best number of dampers and the best damper location.

Bibliographic reference list

1. Koutsoloukas, L., N. Nikitas, and P. Aristidou, *Passive, semi-active, active and hybrid mass dampers: A literature review with associated applications on building-like structures*. elsevier, 2022.
2. Ghaedi, K., et al., *Invited Review: Recent developments in vibration control of building and bridge structures*. JOURNAL OF VIBROENGINEERING, 2017.
3. Bankar, V.K. and A.S. Aradhye, *A Review on Active, Semi-active and Passive Vibration Damping*. International Journal of Current Engineering and Technology, 2016. **6**: p. 2347 – 5161.
4. Higashino, M. and S. Okamoto, *Response Control and Seismic Isolation of Buildings*2006.
5. Hu, J.W., *Response of seismically isolated steel frame buildings with sustainable lead-rubber bearing (LRB) isolator devices subjected to near-fault (NF) ground motions*. Sustainability, 2014. **7**(1): p. 111-137.
6. Nassani, D.E. and M.W. Abdulmajeed, *Seismic Base Isolation in Reinforced Concrete Structures*. International Journal of Research Studies in Science, Engineering and Technology 2015. **2**(2): p. 1-13.
7. M., I., P.D. Metwally, and P.E., *Seismic Isolated Structures: Concept, Review, Design and Worldwide Application*.
8. Åström, K.J. and P. Eykhoff, *System identification a survey*. Automatica, 1971. **7**: p. 123–162.
9. Sarika Radhakrishnan , S.B., *SEISMIC ANALYSIS OF STRUCTURES EQUIPPED WITH X-PLATE METALLIC DAMPERS*. Dept. of of civil engineering, TulsiramjiGaikwadPatilcollege,Maharashtra,India, 2016. **2**(4): p. 2395-4396.
10. Anders, R., *Vibrational Based Inspection of Civil Engineering Structures*, 1993, Aalborg Universitet.
11. FARSANGI, E.N. and A. ADNAN, *Seismic Performance Evaluation of Various Passive Damping Systems in High and Medium-Rise Buildings with Hybrid Structural System*. GU J Sci, 2012. **25**: p. 721-735.
12. Crosby, P., J. Kelly, and J. Singh, *Utilizing visco-elastic dampers in the seismic retrofit of a thirteen story steel framed building*. In Structures Congress, 1994.
13. Soong, T.T. and G.F.D.J. Wiley, *Passive energy dissipation systems in structural engineering* ISBN 0-471-96821-81997, Wiley: May 5, 1997.
14. Chang, K.C., et al., *Seismic behavior of steel frame with added viscoelastic dampers*. Journal of Structural Engineering, 1995. **121**: p. 1418-1426.
15. Symans, M.D. and M. Constantinou, *Passive fluid viscous damping systems for seismic energy dissipation*. Journal of Earthquake Technology, 1998. **35**: p. 185-206.
16. Eltaeb, M., *Active Control of Pendulum Tuned Mass Dampers for Tall Buildings Subject to Wind Load*. Engineering, Environmental Science, 2017.
17. Purohit, A., *A Review of Semi Active Control Algorithms for Magnetorheological (MR) Dampers*. International Journal of Research and Analytical Reviews (IJRAR), 2018. **5**(2): p. 2349-5138.
18. Cheng, F.Y., H. Jiang, and K. Lou., *Smart structures: innovative systems for seismic response control*. CRC press, 2008.
19. Saaed, T.E., *tructural Control and Identification of Civil Engineering Structures*, 2015, Luleå University of Technology.

Bibliographic reference list

20. Kolekar, S., et al., *Preparation of a Silicon oil based Magneto Rheological Fluid and an Experimental Study of its Rheological Properties using a Plate and Cone Type Rheometer*. JOURNAL OF ISSS, 2014. **3**: p. 23-26.
21. Wen, Y.-K., *Method for random vibration of hysteretic systems*. Journal of the engineering mechanics division, 1976. **102**: p. 249-263.
22. Yoshioka, H., J. Ramallo, and B. Spencer, *Smart" Base Isolation Strategies Employing Magnetorheological Dampers*. Journal of Engineering Mechanics-asce - J ENG MECH-ASCE, 2002. **128**.
23. Mehdi , B.-n., et al., *Optimal sliding mode control of single degree-of-freedom hysteretic structural system*. Elsevier, 2012. **17**(11): p. 4455-4466.
24. Franklin, C. and t. peter, *Generalized optimal active control algorithm for nonlinear seismic structures*. Tenth World Conference on Earthquake Engineering, 1992.
25. Saburo, S., et al., *A study of applicability of vibration control to nonlinear structure for seismic excitation*. Tenth World Conference on Earthquake Engineering, 1992.
26. Yang, J.N., et al., *ASEISMIC HYBRID CONTROL OF NONLINEAR AND HYSTERETIC STRUCTURES I*. Journal of Engineering Mechanics, 1992: p. 1423-1440.
27. J, Y., W. J, and A. A, *Sliding mode control for nonlinear and hysteretic structure*. Journal of Engineering Mechanics, 1995. **121**: p. 1330–1339.
28. YANG, J.N., A.K. AGRAWAL, and S. CHEN, *OPTIMAL POLYNOMIAL CONTROL FOR SEISMICALLY EXCITED NON-LINEAR AND HYSTERETIC STRUCTURES*. EARTHQUAKE ENGINEERING AND STRUCTURAL DYNAMICS, 1996. **VOL. 25**: p. 1211-1230.
29. Sivaselvan, M.V. and A.M. Reinhorn, *HYSTERETIC MODELS FOR DETERIORATING INELASTIC STRUCTURES*. JOURNAL OF ENGINEERING MECHANICS, JUNE 2000: p. 633-640.
30. J.C, R., Y. H, and S. B.F, *A Two-Step Identification Technique for Semiactive Control Systems*. Struct. Control Health Monit, 2004. **11**: p. 273-289.
31. Cimellaro, G.P., O. Lavan, and A.M. Reinhorn, *Design of passive systems for control of inelastic structures*. Earthquake Engng Struct, 2009. **38**: p. 783–804.
32. Reinhorn, A.M., O. Lavan, and G.P. Cimellaro, *Design of controlled elastic and inelastic structures*. 2009. **8**: p. 469-479.
33. O, L. and D. GF, *Multi-objective evolutionary seismic design with passive energy dissipation systems*. Journal of Earthquake Engineering, 2009. **13**: p. 758–790.
34. Li, L., G. Song, and J. Ou, *Nonlinear structural vibration suppression using dynamic neural network observer and adaptive fuzzy sliding mode contro*. Journal of Vibration and Control, 2010. **16**: p. 1503–1526.
35. Fabio, M., et al., *Modeling and nonlinear seismic analysis of framed structures equipped with damped braces*. International Conference on Computer Engineering and Applications
2013.
36. Ray, T., A. Reinhorn, and S. Nagarajaiah, *Nonlinear elastic and inelastic spectra with inherent and supplemental damping*. Earthquake Engineering & Structural Dynamics, 2013. **42**: p. 2151–2165.
37. Cimellaro, G.P. and A.M. Reinhorn, *Multidimensional Performance Limit State for Hazard Fragility Functions*. JOURNAL OF ENGINEERING MECHANICS, 2011: p. 47-60.
38. Khansefid, A. and M. Ahmadizadeh, *An investigation of the effects of structural nonlinearity on the seismic performance degradation of active and passive control*

Bibliographic reference list

- systems used for supplemental energy dissipation. Journal of Vibration and Control* 1–11, 2015.
39. Boccamazzo, A., et al., *Seismic effectiveness of hysteretic tuned mass dampers for inelastic structures*. elsevier, 2020: p. 0141-0296.
 40. N.H.Kim, *Introduction to nonlinear finite element analysis*. . Springer Science and Business Media, 2014.
 41. Bouadjadja, S., *Nonlinear Behaviour Analysis of Composite Thin Beams and Plates*, 2020, Université Mohamed Khider - Biskra.
 42. Bouc, R., *A mathematical model for hysteresis*. Acta Acustica united with Acustica, 1971. **24**(1): p. 16-25.
 43. Niola, V., et al., *Nonlinear estimation of the Bouc-Wen model with parameter boundaries: Application to seismic isolators*. Computers & Structures, 2019. **222**: p. 1-9.
 44. Kumar, J.A. and D.S. Sundar, *A numerical study on vibration control of a nonlinear Jeffcott rotor via Bouc-Wen model*. FME Transactions, 2019. **47**(1): p. 190-194.
 45. he;, j. and z.-f. fu, *Modal analysis*. Elsevier, 2001.
 46. Datta, T.K., *Seismic analysis of structures*. Indian Institute of Technology Delhi, India John Wiley & Sons, 2010.
 47. Ogata, K., *Modern Control Engineering*. Prentice Hall, 2010.
 48. Abdeddaim, M., *Contribution à la réduction du risque d'entrechoquement des bâtiments adjacents sous séisme de forte intensité*, 2017.
 49. Kotrane, A., *Conception, réalisation et caractérisation dynamique d'un amortisseur magnéto rhéologique*. École de technologie supérieure, 2007.
 50. Yang, J.N., Z. L, and S. Vongchavalitku, *generalization of optimal control theory : linear and non linear control*. Journal of Engineering Mechanics, 1994. **Vol. 120**: p. 266-283.
 51. J. N. Yang, F.X.L., D. Wong, , *Optimal control of nonlinear Structures*. journal of applied and computational mechanics, 1988. **55**(4): p. 931-938 (8 pages).
 52. J. N. Yang, Z. Li, S. C. Liu,, *ASEISMIC HYBRID CONTROL OF NONLINEAR AND HYSTERETIC STRUCTURES I*. Journal of Engineering Mechanics, 1992. **118**(7): p. 1423-1440.